

Author Response to RC1

Thank you for your useful comments. Our responses to your comments and the comments of the other two reviewers have greatly improve the manuscript. Below are our responses (in blue) to each comment in turn. The lines and page numbers refer to the revised version with tracked changes.

While responding to comments from all reviewers we found a bug in our code in the way we treat asymmetry. As described in the original manuscript, we first remove an estimate of the asymmetry due to forward speed from the input best track V_{max} . The portion removed is a function of the TC translation speed, $V_t = 1.173V_t^{0.63}$, following Chavas et al., (2017). We then add back an estimate of the asymmetry to the spatial 10m wind field diagnosed by KW01, again following Chavas et al., (2017). And in addition, we apply a factor that varies with radial distance from the storm center (the factor is equal to 1 at the radius of maximum winds and then decays with increasing radius) following Jakobsen and Madsen (2004). The bug was that the code missed adding back the V_t -dependent factor and only added back the radially-dependent factor. This caused us to add back the full value of V_t at R_{max} which caused too strong asymmetry, particularly for fast moving storms over Japan for example. In response, original figures 2, 3 and 4 have been corrected. The analysis in original figure 7 is for along-track winds which is not affected by this bug fix.

Chavas, D. R., Reed, K. A. and Knaff, J. A.: Physical understanding of the tropical cyclone wind-pressure relationship. *Nature communications*, 8(1), p.1360, <https://doi.org/10.1038/s41467-017-01546-9>, 2017.

Jakobsen, F. and H. Madsen, H.: Comparison and further development of parametric tropical cyclone models for storm surge modeling. *Journal of Wind Engineering*, 92, 375-391, <https://doi.org/10.1016/j.jweia.2004.01.003>, 2004.

The manuscript proposed a new modeling system for generating tropical cyclone (TC) wind, which consists of a parametric radial profile model, the non-linear boundary layer model (KW01), and the terrain effects. The authors presented a case of hurricane Maria and Wilma and verified the model using landfalling storms. Then, the authors discussed the impact of terrain on the changes of TC winds over the South East US, Taiwan and Eastern China, and Eastern Australia. Overall, I like this approach and can think of many applications of this model. One criticism I have is that the advantage of using KW01 was not shown or discussed with evidence. In Section 2.3, The authors described KW01 as the key advancing component of the modeling system. At many other places, the author says that their system contains more dynamical processes than other existing tools. However, none of the results shown here can isolate the positive impact of using KW01. I suggest conducting additional simulations using Willoughby's wind with an empirical factor applied to get winds at 10m height, plus the terrain effect. By comparing these new simulations with the Willoughby+KW01+terrain, we can see the advantage of (or differences caused by) KW01.

The suggestion to better demonstrate the advantage of using KW01 is a good one. We agree that this is needed, given that we state that the use of KW01 is the main advance of our modeling approach. Section 3 of the revised manuscript has been almost completely rewritten

to better demonstrate the advantage of KW01, and its interactions with surface roughness and topography using the case study of Hurricane Maria (2017) over Puerto Rico.

The new section includes a series of sensitivity simulations to isolate the effect of i) adding the boundary layer model, ii) adding variable surface roughness, and iii) adding variable terrain height. The impacts are presented in plots of surface wind reduction/amplification factors. In addition, a plot of the surface roughness is included to better interpret surface roughness effects. Also, a snapshot of the model output wind field is shown as Maria makes landfall, to show there is no strong deviation of winds around local hills. The full model simulation is also evaluated against available surface station observations.

Regarding adding a simulation that applies an empirical factor to Willoughby, we explored the possibility of calculating wind multiplication factors that account for terrain and topographic effects. A recent summary of wind multiplication factors used by international and national wind engineering codes found large differences in the level of complexity in the approaches and assumptions (Yang et al. 2014). As described in Tan and Fang (2018), calculating the topographic multiplication factor is non-trivial and requires a number of assumptions about the overlapping influence of nearby peaks within complex terrain and how this varies with wind direction. The resulting wind field would then be very sensitive to our assumptions. Developing expertise in constructing topographic multiplication factors is beyond the scope of this study. We therefore leave a comparison of our topographic effect with topographic multiplication factors used in Yang et al. (2014) for future work, as noted on P21, lines 5-6.

In the absence of inland observations an alternative approach to model evaluation is to compare with a simulation using a full atmosphere numerical weather prediction model. We were able to acquire data from a Weather Research Forecasting model simulation of Maria. Our intention was to use this simulation to compare the terrain response of KW01 with the NWP model simulation. However, we found that WRF has a problem with dropping the 10-m winds too much over land and immediately at the coast. Fixing this problem was beyond the scope of this paper.

Tan, C. and Fang, W.: Mapping the wind hazard of global tropical cyclones with parametric wind field models by considering the effects of local factors. *International Journal of Disaster Risk Science*, 9(1), 86-99, <https://doi.org/10.1007/s13753-018-0161-1>, 2018.

Yang, T., Cechet, R.P. and Nadimpalli, K., 2014. *Local wind assessment in Australia: Computation methodology for wind multipliers*. Geoscience Australia. 2014/33.

Below are a few minor comments and questions

1. Page 4, line 2. While I understand the advantage of using KW01 instead of a simple empirical model, this sentence sounds vague. Please elaborate more on what the additional dynamical effects are.

The additional dynamical effects are now discussed on P4, line 30 – P5, line 3.

2. The first paragraph of section 5 (page 11) should belong to Section 2.1.

This paragraph has been moved as suggested.

3. Page 5, Line 15: Please mention the TC boundary layer height used in this study as well. Is the model performance sensitive to the TCBL height?

Page 7, Line 8 states that the model top is held fixed for all simulations at 2km. This was chosen to be above the typical height of super-gradient jets. We also state that *'While the boundary layer height likely varies substantially across global TCs, we choose to keep this fixed in the absence of readily available data'*. We also note that the TCBL height varies strongly with radial distance from the center of a given storm (Kepert et al. 2012). The height also depends on the specific definition of TCBL top. We have not explored sensitivity to our model top, but agree that it is a key parameter that may affect other aspects of model setup such as the factor used to inflate the input best track Vmax from the surface to model top. This unexplored model sensitivity is acknowledged in the conclusions P21, lines 7-8.

Kepert, J. D.: Choosing a boundary layer parameterization for tropical cyclone modelling. *Monthly Weather Review* 140, 1427–1445, <https://doi.org/10.1175/MWR-D-11-00217.1>, 2012.

4. Page 7, L11 'running for 24 hours for each forcing update is computationally impractical.' I am surprised to see that running 24 hours of KW01 is computationally impractical. What is the computational cost of KW01, and how is it compare to the computational cost of 2-km WRF.

I am asking this is because, for assessing wind risk, the most significant advantage of a simplified wind generator v.s. a full-physical model is its low computational cost. If running KW01 is computationally expensive, this system will not be able to use for real risk assessment, which (I thought) is one (and probably the most important one) of motivations of this work. (The other motivation is to understand wind risk over complex terrain using historical cases. For this purpose, we can always run WRF or other mesoscale models which may generate more realistic winds than KW01)

Thank you for raising this important point. The simulation wall-clock time strongly depends on the number of grid points. For the large domains needed to capture the long tracks of fast-moving storms (over Japan or the Northeast U.S., for example) the wall-clock time is substantially longer than using wind profile models alone. The most expensive domain, over Japan, is 900 X 1100 X 18 grid points using 2-km grid spacing and a 2 second timestep. A 24-hour simulation took 6 hours wall-clock time on 36 cores. Smaller domains run at 4km run much quicker.

Running a 24-hour period for a single event is therefore computationally quite practical. But running for 24 hours for each 10-minute forcing update to ensure full equilibrium is reached for each forcing update would rapidly increase computational demands to impractical levels.

Running the WRF model over the same domain would cost more due to the higher number of vertical levels, and a greater number of physical processes. We have not run WRF over these specific domains so we are not able to provide a computational cost. Even if it were feasible to run WRF for all 714 historical cases simulated here, future applications of our modeling approach to large numbers of synthetic TC tracks would presumably become impractical for WRF.

A short discussion of the computational cost of our modeling approach has been added to the conclusions section, P19, lines 9-14.

5. Page 9, L24. Do you mean the maximum wind speed recorded at the station during the lifetime of the storm, which is different from the storm lifetime maximum wind speed (which is usually one value per storm)?

We don't see this specifically mentioned on page 9, L24. But your point is correct. We do indeed mean the max wind speed recorded at the station during the lifetime of the storm. This point has been corrected throughout the manuscript.

6. Page 11, L1: Where is this 20% bias correction factor coming from? Is it universally applied to all simulations?

On further consideration, and in response to similar concerns from other reviewers, we decided to remove this bias correction factor from this study. The original factor of 20% was determined by comparing our simulations with surface station data in urban areas for a subset of 8 landfalling U.S. hurricanes. This bias correction step was added to aid application of the dataset but clearly patches over an underlying problem.

Holmes (2007) found that the roughness length for urban areas can vary between 0.1 and 0.5m for suburban regions and rise to between 1 and 5m for densely packed high-rises in urban centers. Our model uses a single roughness length for all urban areas (suburban and city centers) of 0.8m and this was taken from the MODIS land use dataset – the same as used in the Weather Research and Forecasting (WRF) model. This value is too high for suburban areas, where a value closer to 0.2 is typical (Yang et al. 2014). Depending on the specific siting of the wind observing stations, it's probable that the introduction of multiple urban categories with different roughness lengths would improve our low wind speed bias. This detailed investigation is beyond the scope of this paper and we choose to leave this for future work. The revised manuscript includes a discussion on P14, lines 7-12.

Holmes, J. D., 2007. Wind loading of structures. 2nd ed. London and New York, Taylor & Francis

Yang, T., Cechet, R.P. and Nadimpalli, K., 2014. *Local wind assessment in Australia: Computation methodology for wind multipliers*. Geoscience Australia. 2014/33.

7. Page 11. L12-14 belongs to the figure caption of Fig. 6, not in the main text.

This text has been moved to the figure caption of Fig. 5 (the figure that shows all domains).

8. Figure 7 and the related discussion. Did you check the enhanced vertical diffusion and vertical advection in KW01? Can you show some analysis of these enhanced features? There is a lag between the terrain and the wind gradient. Why?

Figure 7 shows how the inland gradient of wind speed varies with distance inland from the coast, together with the terrain height. The gradient of wind speed and the terrain height is the along-track average over all simulated storms by region. The gradient of the wind speed is also the net effect of not just topography but also variations in surface roughness and the overall

inland decay according to the input best track Vmax. This makes it challenging to isolate the processes driving the inland wind speed gradient. This complexity has been highlighted in the revised manuscript on P17, lines 22-27, and we have changed our asserted mechanism to be a suggested mechanism.

Carefully constructed idealized experiments would be needed to isolate the processes (enhanced vertical diffusion and vertical advection in KW01) driving wind acceleration on the upwind slopes and crests of terrain features. We choose to leave this investigation for another study that would focus more on the process-level understanding rather than a global assessment as presented here. This point is noted in the conclusions.

The distance-rate-of-change in wind speed shows increases (or for some regions, a lessening of the inland decay) along the upwind slopes up to the crest (where, for example in Fig. 7b the wind gradient switches from positive to negative). The lee sides show some evidence of accelerated inland wind decay. This is similar to the topographic effect on the winds shown for the single storm Maria in Fig. 2. We don't see a strong lead-lag effect.

9. Willoughby et al. 2006 is missing in the references.

Thank you for spotting this oversight. The reference has been added.

Author Response to RC2

Thank you for these useful comments and list of references. Our responses to your comments and the comments of the other two reviewers have greatly improve the manuscript. Below are our responses (in blue) to each comment in turn. The lines and page numbers refer to the revised version with tracked changes.

While responding to comments from all reviewers we found a bug in our code in the way we treat asymmetry. As described in the original manuscript, we first remove an estimate of the asymmetry due to forward speed from the input best track V_{max} . The portion removed is a function of the TC translation speed, $V_s=1.173V_t^{0.63}$, following Chavas et al., (2017). We then add back an estimate of the asymmetry to the spatial 10m wind field diagnosed by KW01, again following Chavas et al., (2017). And in addition, we apply a factor that varies with radial distance from the storm center (the factor is equal to 1 at the radius of maximum winds and then decays with increasing radius) following Jakobsen and Madsen (2004). The bug was that the code missed adding back the V_t -dependent factor and only added back the radially-dependent factor. This caused us to add back the full value of V_t at R_{max} which caused too strong asymmetry, particularly for fast moving storms, over Japan for example. In response, original figures 2, 3 and 4 have been corrected. The analysis in original figure 7 is for along-track winds which is not affected by this bug fix.

Chavas, D. R., Reed, K. A. and Knaff, J. A.: Physical understanding of the tropical cyclone wind-pressure relationship. *Nature communications*, 8(1), p.1360, <https://doi.org/10.1038/s41467-017-01546-9>, 2017.

Jakobsen, F. and H. Madsen, H.: Comparison and further development of parametric tropical cyclone models for storm surge modeling. *Journal of Wind Engineering*, 92, 375-391, <https://doi.org/10.1016/j.jweia.2004.01.003>, 2004.

Review of “Modelling Global Tropical Cyclone Wind Footprints” by James M. Done et al.

Summary

The MS describes a method for automated modelling of tropical cyclone winds, both instantaneous fields and the maximum wind swath over the life of the storm. An axisymmetric representation of the gradient-level wind is derived using inputs from, for example, a best track database. Then a nonlinear boundary-layer model is used to calculate the winds throughout the boundary layer, including at the surface (10 m), from this gradient-level wind, accounting for storm motion, heterogeneous surface roughness and topography.

There are three potentially serious flaws with this approach, relating (i) to the way the parametric profile of Willoughby et al (2006) has been used, (ii) to the likely inability of the nonlinear tropical cyclone boundary layer model to correctly model mountain waves, and (iii) to the authors’ misapplication of the work of Harper et al (2010) in adjusting observed winds for different averaging periods. These are expanded upon below. In addition, some minor points where clarification is needed are noted.

Use of the Willoughby et al. (2006) parametric profile

The criticism here is not that the authors have chosen this profile – indeed, I consider it to be the most suitable tropical cyclone parametric profile presently available, because of its superior ability to fit observations. Rather, it is criticism of the way they have used it. The authors note that in section 2.2 that the “Holland et al. (2010) profile has the advantage of tying down the radial decay profile using an observation of an outer wind, say the radius of 34 knot winds” and go on to note that such observations are not always available. They then note that the Willoughby et al. (2006) profile has two exponential decay scales for the outer part of the vortex. In addition, the user must assign the relative weight of these two profiles, so there are three free parameters that determine the shape of the vortex outside of the radius of maximum winds (RMW), although in practice Willoughby et al.

(2006) recommends that one length scale be held fixed at 25 km. Choosing values for the remaining two free parameters requires additional data; Kepert (2006a,b) and Schwendike et al. (2008) describe the use of aircraft reconnaissance data for this purpose and discuss the associated difficulties. This choice can lead to substantial differences in the shape of the wind profile and hence the radius of gales, and Willoughby et al. (2006) show that a wide range of the second length scale occurs in nature, with their Fig 11 showing it can range from about 100 km to over 450 km. The authors of the MS under review not only omit to describe how they have chosen these crucial parameters; they also incorrectly assert that the Willoughby et al (2006) profile has “fewer required data inputs”.

Thank you for this informed comment on our use of the Willoughby et al. (2006) parametric profile. We have removed the assertion that the Willoughby et al. (2006) profile requires fewer data inputs than the Holland et al. (2010) profile.

We agree that the outer radius of damaging winds can be highly sensitive to the choice of the free parameters. We did not provide sufficient detail on how the three free parameters are chosen. The revised manuscript now explains our choices in Section 2.2.

Firstly, we state that the length scale for the transition region across the eyewall is set to 25km when R_{max} is greater than 20km and is set to 15km otherwise. For the shape of the vortex outside R_{max} , we hold the faster decay length scale fixed at 25km, following the recommendation of Willoughby et al. (2006), and allow the second length scale ($X1$) and the contribution of the fast decay rate (A) to vary the shape of the profile. For the slower decay length scale, we note that Willoughby et al. (2006) showed that a wide range of the second length scale occurs in nature, with their Fig. 11 showing it can range from about 100 km to over 450 km. We also note the difficulties in using aircraft reconnaissance data for this purpose (as in Kepert 2006a,b and Schwendike et al. 2008). Given that aircraft data are not uniformly available globally, and our intention to only use readily available data, we decide not to include these additional data sources for subsets of global historical events. Willoughby et al. (2006) demonstrated dependence on V_{max} , and latitude, with the more intense low latitude TCs being more sharply peaked. We also have R_{max} readily available. We therefore choose to allow the remaining two free parameters (A and $X1$) to vary with readily available parameters R_{max} , V_{max} and latitude, following equation 11 in Willoughby et al. (2006). This globally consistent approach is needed to allow relative risk assessments across regions.

Use of the Kepert and Wang (2001) nonlinear tropical cyclone boundary layer model

This model, and others like it, are the most sophisticated diagnostic models of the tropical cyclone boundary-layer presently available. However, there are two important areas in which the authors have failed to establish that their use of the model is appropriate.

Firstly, the model as originally formulated was written in storm-following coordinates. This enabled the efficient simulation of moving storms, since a smaller domain could be used, and indeed Kepert and Wang (2001) remains one of the few theoretical papers on the tropical cyclone boundary layer to consider the effects of storm motion. The authors describe some modifications to the model, which they state are to allow for a time-varying gradient wind field, and for landfall. While their description is unclear, it appears that they may have changed to earth-relative coordinates, for they

state that “a translation vector is added to the horizontal advection terms in KW01”. Unfortunately, the governing equations are omitted, so it is impossible to be sure. However, they do note that “the proportion of the translation vector added reduces close to the surface due to surface friction”. This is certainly incorrect; the whole of the coordinate system must move with the same velocity! Perhaps it is an attempt to allow for friction in the environmental flow, which the model (in its original form) assumes is equal to the translation vector. However, whether in earth-relative or storm-relative coordinates the model should be able to spin up the boundary layer of any environmental flow, and if in storm-relative coordinates does not require the addition of a translation vector. Perhaps the authors’ modification is correct, but until they give equations this cannot be established, and as outlined above, their description doesn’t sound correct.

Thank you for this comment. We agree that our original description was unclear. We also apologize for including some old and incorrect description of the model setup. The few lines of incorrect description was a legacy of some earlier model development and testing. The revised manuscript more clearly and accurately describes the final modeling approach that we settled on (Section 2.3).

The original model coordinates of KW01 were storm-relative. The storm in this original coordinate system therefore did not move by definition. To account for the effect of storm motion, the original model includes the pressure gradient of the environmental flow in the forcing pressure profile at the model top.

We changed the model to run in Earth-Relative coordinates. Each simulation is conducted on one of the 17 geographically-fixed regional domains shown in Fig. 5. Our early model testing retained the effect of forward speed in the forcing of KW01 but we found KW01 strongly damped the asymmetry and we did not have the resources to find the cause. We therefore chose to take out the effect of forward speed from the forcing for KW01 and treat it in pre- and post-processing steps as depicted in the workflow shown in original Fig. 1. We also do not add the translation vector to the horizontal advection terms. That was a mistake in our description so thank you for pointing that out.

Our approach therefore misses any interaction effects between terrain and the asymmetrical component of the storm wind field. The importance of these effects are unknown and we leave their inclusion for a future iteration of our model.

I note also that, since the Kepert and Wang (2001) model incorporates the effects of translation, the postprocessing step of adding on a motion asymmetry shown in Figure 1 is at best unnecessary, but most likely also incorrect.

As noted in our response above, we removed the effects of translation from KW01. Adding on a motion asymmetry was therefore necessary.

The second issue concerns the possibility of mountain wave activity. The model does allow for surface topography, although this facility has not before been the subject of published papers to my knowledge. However, it is unlikely it would accurately represent mountain wave activity, because of the shallow depth of the domain – modelling studies of mountain waves typically consider at least the full depth of the troposphere. Although some of the discussion in the introduction could be interpreted as evidence against mountain waves, it is far from rigorous – for instance, the authors note that the Froude number will be high without considering that this will also depend on the flow geometry. In addition, they note the

“quasi-neutral stability”; while this is plausible near the eyewall provided one considers moist stability, it is incorrect at larger radius as shown by the observational composites of Zhang et al. (2011).

Thank you for this useful comment. We can see how our discussion of full NWP model simulations by Ramsay and Leslie (2008) may have been interpreted as an indication that mountain wave activity was represented in our modeling approach. Our model top at 2-km cuts off the free troposphere needed for large-scale mountain waves that can bring free-atmosphere winds down to the surface. It’s also unlikely that our model has the resolution to capture flow-separation turbulence downwind of crests and escarpments.

The revised manuscript more clearly articulates the physical terrain effects permitted by the model (P4, line 30 – P5, line 3). These include convergence, vertical diffusion and vertical advection on windward slopes and crests resulting in locally strong low-level shear and TKE production. In addition, the vertical boundary layer structure allows the potential for super-gradient jets (Franklin et al. 2003; Kepert and Wang 2001) to influence winds in high terrain. Finally, the time dimension allows for upwind effects due to upwind terrain variations and terrain to be incorporated.

In the revised manuscript, our discussion of the Froude number acknowledges the contribution of mountain geometry (P3, lines 12 - 13). For high mountains, the wind has a greater potential to become blocked. On closer inspection we didn’t see any evidence of substantial blocking (upstream deceleration) in any of our runs. This is discussed further for the case of Maria over Puerto Rico in the expanded Fig. 2. We also now acknowledge that our modeling approach doesn’t directly allow any blocking to affect the TC track, although the observed tracks that are used do include such blocking effects (P19, lines 9-12).

We agree that a neutral boundary layer is not guaranteed at large radii. Kepert (2012) indicates increasing static stability as subsidence increases at these larger radii. Even so, measurements of turbulent fluxes in high-wind environments between outer rain bands by Zhang et al. (2009) find shear production and dissipation to be the dominant source and sink terms of TKE. This is noted in the revised manuscript on P3, lines 15-17.

Zhang, J. A., W. M. Drennan, P. G. Black, and J. R. French, 2009: Turbulence structure of the hurricane boundary layer between the outer rainbands. *J. Atmos. Sci.*, 66, 2455–2467

Conversion of wind speed averaging periods

The authors have adjusted surface wind observations for averaging period, claiming as justification the work of Harper et al. (2010). This is incorrect. Harper et al. (2010) emphasise that their conversion factors are to be used for tropical cyclone intensity, and that they should **not** be used for wind observations. Please refer to the third paragraph of the executive summary, section 1.3 and appendix E of that report.

We understand that the shorter averaging period can only be considered a gust in the context of a longer averaging period over which the wind is considered steady (i.e., constant variance/turbulence). Estimating the 1-minute ‘gust’ from buoy-observed 10-minute mean wind should therefore be appropriate. But estimating the 1-minute ‘gust’ from the surface station-observed 2-minute wind is questionable since the 2-minute wind is not necessarily a measure of the mean wind. This 2-minute wind could be higher or lower than the true mean wind.

However, we still desire to use these 2-minute observations for model evaluation. We therefore choose to use the factor to estimate the 1-minute wind from the 2-minute wind, despite the inconsistency with statistical theory. In this, we assume that errors arising from this factor application are i) similar in magnitude to the uncertainty in the definition of the 1-minute wind from numerical model data, and ii) similar to errors due to gusts deviating from statistical theory due to winds not in equilibrium with the variable surface conditions.

Further comments

Page 3 line 2, the Willoughby et al (2006) profile is not intended for surface winds.

In the revised manuscript we more accurately state that the Holland et al., (2010) profile, for example, models the surface winds directly whereas the Willoughby et al., (2006) profile models the gradient-level winds and an extra step is needed to determine the surface winds (P3, lines 29-31).

Page 5 line 8, and elsewhere, the authors claim to use an “average value of R_{max} around the storm”. This seems strange, R_{max} is usually not regarded as having significant asymmetries, unlike say R34.

This comment about taking an average value of R_{max} around the storm has been removed.

Page 5 line 16, 500 m is too low here, as it is either at or below level of the supergradient jet.

We have changed this to be consistent with the definition of boundary layer height based on the depth of the inflow. We now explain that ‘One definition for the boundary layer height is the depth of the inflow, defined as the height where the radial inflow falls to 10% of the peak inflow. Using radiosonde ascents in 13 hurricanes Zhang et al., (2011) find this height to be approximately 850m at the radius of maximum wind rising to approximately 1300m at larger radii.’ (P7, lines 8-10).

Page 6 line 8, the value of the eyewall surface wind factor of $1/1.32 = 0.75$ is high compared to observations (Franklin et al. 2003, Powell et al. 2009) and theory (Kepert and Wang 2001).

Franklin et al. (2003) observed an inner core wind maximum at about 500m that increases to about 1km for the outer winds. They found a logarithmic profile below the wind maximum and a reduction of winds above due to the warm core. The result is a 700-hPa-to-surface wind factor of about 0.9 in the inner core. Kepert and Wang (2001) theory also has a factor of 0.9 in the inner core, with the factor decreasing to 0.75 in the outer winds. Knaff et al. (2011) took the Franklin et al. (2003) factor of 0.9 in the inner core and additionally reduced it by a factor of 0.8 to go from marine-exposure winds to terrestrial-exposure winds, giving a net factor of $0.9 \times 0.8 = 0.72$.

Initial testing using a variable factor for offshore and onshore track caused enhanced winds just offshore in response to the higher factor for the first inland track point. This is because the outer winds were still responding to the low surface roughness while being driven by stronger gradient winds. We therefore choose to hold the factor fixed and appropriate for inland winds.

This is now discussed in the revised manuscript at the end of Section 2.2.

Knaff, John A, Mark DeMaria, Debra A Molenaar, Charles R Sampson, and Matthew G Seybold. 2011. “An Automated, Objective, Multiple-Satellite-Platform Tropical Cyclone Surface Wind Analysis.” *Journal of Applied Meteorology and Climatology* 50 (10): 2149–66.

Page 6 line 31, the Kepert and Wang (2001) model cannot resolve turbulence, since it uses a fixed pressure field. In this, it is unlike recent high-resolution simulations of tropical cyclones by Nolan et al. (2014) and Stern and Bryan (2018).

We agree that Kepert and Wang (2001) cannot resolve turbulence, but it does parameterize the effects of turbulence through its turbulence scheme. This is now more clearly stated on P9, line 7.

Page 7 line 2, the model does represent buoyancy, although probably not particularly well since it ignores moist processes.

The revised manuscript more correctly states that the model does not represent buoyancy *well* (P9, line 8). But for most TCs, and for the inner core region of the strongest winds, we expect buoyancy effects to be small.

Page 9 line 12, it is unclear how figure 3a shows this correction.

In response to the concerns of the other two reviewers we decided to remove this 20% correction factor from this study. The original factor of 20% was determined by comparing our simulations with surface station data in urban areas for a subset of 8 landfalling U.S. hurricanes. This bias correction step was added to aid application of the dataset but clearly patches over an underlying problem.

Holmes (2007) found that the roughness length for urban areas can vary between 0.1 and 0.5m for suburban regions and rise to between 1 and 5m for densely packed high-rises in urban centers. Our model uses a single roughness length for all urban areas (suburban and city centers) of 0.8m and this was taken from the MODIS land use dataset – the same as used in the Weather Research and Forecasting (WRF) model. This value is too high for suburban areas, where a value closer to 0.2 is typical (Yang et al. 2014). Depending on the specific siting of the wind observing stations, it's probable that the introduction of multiple urban categories with different roughness lengths would improve our low wind speed bias. This detailed investigation is beyond the scope of this paper and we choose to leave this for future work. A discussion on this point has been added P14, lines 7-12.

Holmes, J. D., 2007. Wind loading of structures. 2nd ed. London and New York, Taylor & Francis

Yang, T., Cechet, R.P. and Nadimpalli, K., 2014. *Local wind assessment in Australia: Computation methodology for wind multipliers*. Geoscience Australia. 2014/33.

Page 11 line 1 and in the conclusions, the claim that the model shows “no large bias” in urban areas seems optimistic. At a radius of 300 km, the bias is about -10 m/s. At this radius, this is likely well over half the observed wind speed, hardly negligible!

We agree that stating “no large bias” is not accurate. In response (and in response to another reviewer's comment) we have changed this to state that the model compares well with a recently published global wind swath modeling approach (Tan and Fang, 2018). (P13 lines 28-30). Their approach using similar quantities of input data and local wind multiplication factors to account for terrain features also showed typical errors of 8 to 10m/s. See their Fig. 6 that shows comparison with observations for 36 TCs during 1970–2014 for 25 stations in Hainan Island, China.

Tan, C. and Fang, W.: Mapping the wind hazard of global tropical cyclones with parametric wind field models by considering the effects of local factors. *International Journal of Disaster Risk Science*, 9(1), 86-99, <https://doi.org/10.1007/s13753-018-0161-1>, 2018.

The term “storm lifetime maximum wind” is generally used to refer to the wind swaths (e.g. page 13 line 8) but is ambiguous since it could also refer to the storm’s peak intensity. In this part of the MS, these maximum winds will generally not occur at the storm centre, but they are analysed in terms of along-track distance. How is this calculated?

Thank you for raising this important distinction, that another reviewer also noted. We agree that although we used common definitions, they are rather imprecise. Our use of ‘storm lifetime maximum wind’ refers to the maximum wind speed recorded at a specific location (grid point or observing station location) throughout the lifetime of the storm. The revised manuscript is now more specific whenever this term is used.

For Fig. 7 specifically, wind data are extracted from the wind swath at the location of the TC track. This data is therefore the storm lifetime maximum wind speed at the specific locations along the TC track. Then we composited all TC tracks for a given region about their track points of landfall, and took an average over all tracks. This gives the region-average along-track wind swath vs. distance inland. This calculation is described more clearly in the revised manuscript (P17, lines 7-10).

References

- Franklin, J. L., M. L. Black, and K. Valde, 2003: GPS dropwindsonde wind profiles in hurricanes and their operational implications. *Wea. Forecasting*, 18, 32–44.
- Harper, B. A., J. D. Kepert, and J. D. Ginger, 2010: Guidelines for converting between various wind averaging periods in tropical cyclone conditions, WMO/TD-No. 1555. World Meteorological Organisation, 64 pp.
- Kepert, J. D. and Y. Wang, 2001: The dynamics of boundary layer jets within the tropical cyclone core. Part II: Nonlinear enhancement. *J. Atmos. Sci.*, 58, 2485–2501.
- Kepert, J. D., 2006: Observed boundary–layer wind structure and balance in the hurricane core. Part I: Hurricane Georges. *J. Atmos. Sci.*, 63, 2169–2193. doi:10.1175/JAS3745.1
- Kepert, J. D., 2006: Observed boundary–layer wind structure and balance in the hurricane core. Part II: Hurricane Mitch. *J. Atmos. Sci.*, 63, 2194–2211. doi:10.1175/JAS3746.1
- Nolan, D. S., J. A. Zhang and E. W. Uhlhorn, 2014: On the limits of estimating the maximum wind speeds in hurricanes. *Mon. Wea. Rev.*, 142, 2814 – 2837. doi:10.1175/MWR-D-13-00337.1
- Powell, M. D., P. J. Vickery, and T. A. Reinhold, 2003: Reduced drag coefficient for high wind speeds in tropical cyclones. *Nature*, 422, 279–283.
- Schwendike, J. and J. D. Kepert, 2008: The boundary–layer winds in Hurricanes Danielle (1998) and Isabel (2003). *Mon. Wea. Rev.*, 136, 3168–3192.
- Stern, D. P. and G. H. Bryan, 2018: Using Simulated Dropsondes to Understand Extreme Updrafts and Wind Speeds in Tropical Cyclones. *Mon. Wea. Rev.*, 146, 3901 – 3925. doi:10.1175/MWR-D-18-0041.1
- Willoughby, H. E., R. W. R. Darling, and M. E. Rahn, 2006: Parametric representation of the primary hurricane vortex. Part II: A new family of sectionally continuous profiles. *Mon. Wea. Rev.*, 134, 1102–1120.

Zhang, J. A., R. F. Rogers, D. S. Nolan, J. Marks, and D. Frank, 2011: On the characteristic height scales of the hurricane boundary layer. *Mon. Wea. Rev.*, 139, 2523–2535, doi:10.1175/MWR-D-10-05017.1.

Dear Bruce Harper

Thank you for your in-depth and informed comments. Our responses to your comments and the comments of the other two reviewers have greatly improved the manuscript. Below are our responses (in blue) to each comment in turn. The lines and page numbers refer to the revised version with tracked changes.

While responding to comments from all reviewers we found a bug in our code in the way we treat asymmetry. As described in the original manuscript, we first remove an estimate of the asymmetry due to forward speed from the input best track V_{max} . The portion removed is a function of the TC translation speed, $V_t = 1.173 V_t^{0.63}$, following Chavas et al., (2017). We then add back an estimate of the asymmetry to the spatial 10m wind field diagnosed by KW01, again following Chavas et al., (2017). And in addition, we apply a factor that varies with radial distance from the storm center (the factor is equal to 1 at the radius of maximum winds and then decays with increasing radius) following Jakobsen and Madsen (2004). The bug was that the code missed adding back the V_t -dependent factor and only added back the radially-dependent factor. This caused us to add back the full value of V_t at R_{max} which caused too strong asymmetry, particularly for fast moving storms over Japan for example. In response, original figures 2, 3 and 4 have been corrected. The analysis in original figure 7 is for along-track winds and so is not affected by this bug fix.

Chavas, D. R., Reed, K. A. and Knaff, J. A.: Physical understanding of the tropical cyclone wind-pressure relationship. *Nature communications*, 8(1), p.1360, <https://doi.org/10.1038/s41467-017-01546-9>, 2017.

Jakobsen, F. and H. Madsen, H.: Comparison and further development of parametric tropical cyclone models for storm surge modeling. *Journal of Wind Engineering*, 92, 375-391, <https://doi.org/10.1016/j.jweia.2004.01.003>, 2004.

Bruce Harper

The authors seek to “to advance our understanding of overland wind risk in regions of complex terrain and support wind risk assessments in regions of sparse historical data” through the application of a combination of analytical, numerical and empirical techniques. The authors make reference to many very successful more simplified approaches that have been developed over the past three decades that emanate from wind engineering, atmospheric science and insurance loss initiatives. They put the case that previous approaches, in their assessment, lack the essential capacity to incorporate complex terrain and “the essential dynamics and physics” of tropical cyclone (TC) behaviour where “the accuracy of wind speeds over urban (sic) is of critical importance”. The use of a diagnostic 3D numerical boundary layer model is central to their thesis.

While the desirability of such an approach can be supported, where practical, it is ironic that the demonstrated model skill is so poor at reproducing recent historical TC winds in areas where there is a significant amount of quality data available and in mostly flat landscapes. In no way does the model “compare favourably” with the displayed data. An 8 to 10 m/s error band in any hindcast event intended to assist, for example, offshore engineering design or sensitive onshore high-rise design, would be regarded as completely unacceptable. For insurance losses where damage is noted by the authors to

be additionally highly nonlinear with wind speed, it would be massively unreliable. The stated need to apply an empirical "20% adjustment for urban areas" is not only completely inconsistent with the theoretical high ground being argued but is symptomatic of a modelling system that has some significant problems.

As you state below, the challenge of developing a globally applicable approach is that the accuracy at the individual event level will be poorer than for a model developed for individual events or specific regions. This means that for our model evaluation for the subset of observation-rich storms over the U.S. we do not expect that our model should be able to compete with individual event-level approaches that assimilate far more observational data. A globally applicable approach has a number of unique benefits that derive from its small amount of required input data and physical response of the boundary layer winds to terrain. These benefits include generating events in data sparse-regions, generating synthetic events, and application to downscaling TC tracks from global climate models. The case for a global approach has been made stronger in the revised manuscript (P19, lines 26-31).

We note that recently published work that used similar quantities of input data and local wind multiplication factors to account for terrain features (Tan and Fang, 2018) also showed typical errors of 8 to 10m/s. Their Fig. 6 shows comparison with observations for 36 TCs during 1970–2014 for 25 stations in Hainan Island, China. They show 8 to 10m/s errors are typical in the 10-minute sustained winds. Our approach therefore compares favorably with another global modeling approach.

In addition, we also note this magnitude of error are also present in hurricane surface wind vectors utilizing C-band dual-polarization synthetic aperture radar observations, when compared to collocated QuikSCAT-measured wind speeds. For the case of Hurricane Bill Zhang et al. (2014) (Their Fig. 9a and 9b, copied here below) shows scatter (over the ocean) similar in magnitude to our scatter.

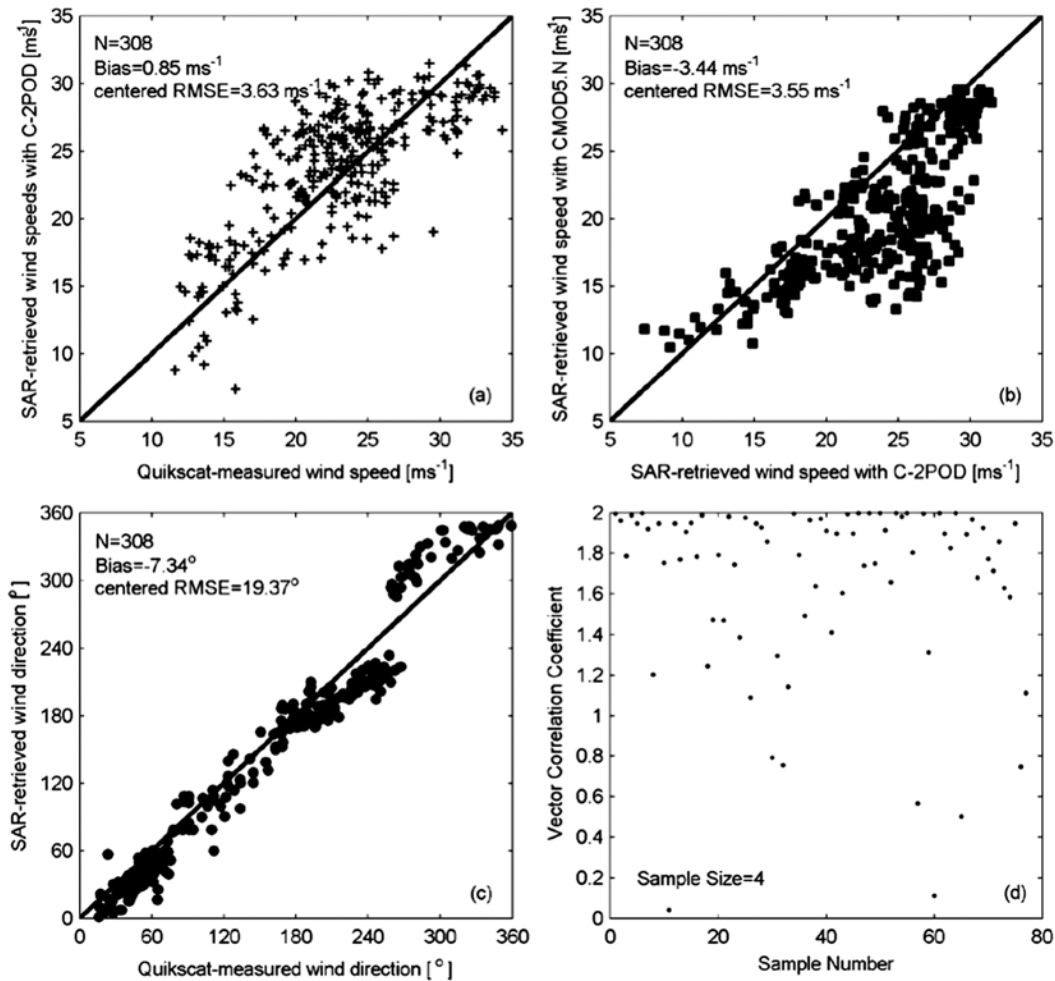


Fig. 9. (a) SAR-retrieved wind speeds from the C-2POD model vs QuikSCAT-measured wind speeds, (b) SAR-retrieved wind speeds from the CMOD5.N model vs from the C-2POD model, (c) SAR-retrieved wind directions vs QuikSCAT-measured wind directions, and (d) vector correlation of wind directions from SAR and QuikSCAT (sample size is 4). Hurricane Bill winds from SAR and QuikSCAT are acquired at 2226 and 2254 UTC 22 Aug 2009, respectively.

The revised manuscript has toned down the assertion that our model compares favorably with observations and now states that it compares favorably with recently published work (Abstract lines 6-7; P13 lines 28-32).

Tan, C. and Fang, W.: Mapping the wind hazard of global tropical cyclones with parametric wind field models by considering the effects of local factors. *International Journal of Disaster Risk Science*, 9(1), 86-99, <https://doi.org/10.1007/s13753-018-0161-1>, 2018.

Zhang, B., Perrie, W., Zhang, J.A., Uhlhorn, E.W. and He, Y., 2014. High-resolution hurricane vector winds from C-band dual-polarization SAR observations. *Journal of Atmospheric and Oceanic Technology*, 31(2), pp.272-286.

We agree that our use of a 20% correction factor for winds over urban areas is weak. On further consideration, and in response to similar concerns from other reviewers, we decided to remove this bias correction factor from this study. The original factor of 20% was determined by comparing our simulations with surface station data in urban areas for a subset of 8 landfalling

U.S. hurricanes. This bias correction step was added to aid application of the dataset but clearly patches over an underlying problem.

Holmes (2007) found that the roughness length for urban areas can vary between 0.1 and 0.5m for suburban regions and rise to between 1 and 5m for densely packed high-rises in urban centers. Our model uses a single roughness length for all urban areas (suburban and city centers) of 0.8m and this was taken from the MODIS land use dataset – the same as used in the Weather Research and Forecasting (WRF) model. This value is too high for suburban areas, where a value closer to 0.2 is typical (Yang et al. 2014). Depending on the specific siting of the wind observing stations, it's probable that the introduction of multiple urban categories with different roughness lengths would improve our low wind speed bias. This detailed investigation is beyond the scope of this paper and we choose to leave this for future work. This point is mentioned on P14 lines 7-12.

Holmes, J. D., 2007. *Wind loading of structures*. 2nd ed. London and New York, Taylor & Francis

Yang, T., Cechet, R.P. and Nadimpalli, K., 2014. *Local wind assessment in Australia: Computation methodology for wind multipliers*. Geoscience Australia. 2014/33.

The Challenge of a Global Approach and the Expected Benefits

The problem with developing tools for global application unfortunately means that accuracy is inevitably impacted by the need to adopt spatially and/or temporally compromised globally available datasets. This situation limits, and actively dissuades, examination of the myriad of fine scale site-specific influences on the TC surface wind during a specific event that cannot be ignored. These have traditionally been transparently handled by reference to standard exposure and application of statistically based boundary layer turbulence approaches. The authors' more complex and computationally demanding approach needs to demonstrate at least a comparable utility.

Please see our comment above. Our approach shows comparable utility to a recently published globally applicable approach that combines parametric wind profile modeling with local wind multiplication factors.

In any case, it is not clear what practical application there is in producing such a global (deterministic) event set, given that the essential need is for risk management that implicitly requires a probabilistic approach. Cherry-picking of historical events does not yield firm statistical guidance and any such results will most likely be less reliable than any regional wind speed risk assessment that is based on (even sparse) long term data sets, given that aggregation of sites is often justified. In spite of the practical challenges in this space, the various engineering design standards around the world have overtime assembled realistic and likely suitably conservative wind risk frameworks, all of which embody the need to allow for height, terrain and topography effects.

A deterministic event set is of significance importance to the risk management industry for two reasons. Firstly, it allows for the validation of the wind field module of tropical cyclone catastrophe models (probabilistic approach). This module is a critical component of these models, and they do not use a physical model for representing the wind speed and rely on site coefficients to represent friction and topography. The module is used to generate stochastic wind fields and historical wind fields for a selection of events. A global deterministic event set based on a

physical model is therefore an excellent tool for validating catastrophe model's wind module via a comparison of historical wind footprints. Secondly, modelling as-if losses from historical storms is a widely used approach to stress test reinsurance structures to ensure companies have adequate protection, and can also be used in submissions to regulators. A global event set is an excellent basis for building scenarios to test as-if losses. These points are now included in the revised manuscript, P2, line 29 – P3 line 2.

The model's development is touted as valuable for insurance-related purposes. However, the principal cause of increasing world-wide losses for insurers is, together with uninformed risk-based planning, the failure to implement known good design, construction and inspection practices for residential development. The importance of globally modelling large scale terrain influences is also overstated given that, compared with typically nearly-flat or undulating conurbations, there is negligible insurance exposure to wind hazard in areas of very high or steep terrain.

We fully agree that one of the principal causes of increasing losses is poor implementation of known good construction practices. Indeed, Simmons et al. (2018) quantified the importance of a strong and well enforced wind building code for reducing insured wind losses in Florida.

There is an industry need for ever more accurate modelling of risk, often for single sites. Representing terrain influences is well known to influence wind speed, and mountainous countries often have both a high risk of tropical cyclones and significant insurance exposure, for example the Philippines and Japan. Therefore we believe an accurate representation of the influence terrain is very important, it is also included in all recent respected proprietary catastrophe models. This point is made in the revised manuscript, P2 lines 27-29.

Simmons, K.M., Czajkowski, J. and Done, J.M., 2018. Economic effectiveness of implementing a statewide building code: the case of Florida. *Land Economics*, 94(2), pp.155-174.

Comments on Method

(2.) The step that “removes an estimate of the asymmetry due to storm motion” from the surface wind relies on the assumption that historical Vmax do reliably include such an influence. While Dvorak, for example, implies that is the case there is no specific allowance in the methodology. Hence the adopted empirical adjustment likely has little merit in terms of overall accuracy.

This is an important point. We agree that the extent to which asymmetry due to forward speed is included in best track estimates of Vmax may be questionable. But given that these winds are Earth-relative measurements we assume that the benefits of removing an uncertain estimate of asymmetry outweighs the cons of not doing so. In this assumption, we follow the approach of others (e.g., Chavas et al. 2017). This point is made in the revised manuscript, P5, lines 16-18.

Chavas, D. R., Reed, K. A. and Knaff, J. A.: Physical understanding of the tropical cyclone wind-pressure relationship. *Nature communications*, 8(1), p.1360, <https://doi.org/10.1038/s41467-017-01546-9>, 2017.

In quoting Harper, Kepert and Ginger (2010) (aka the WMO wind averaging guidelines - hereafter HKG), the assumption that numerically modelled winds calculated at a small timestep are representative of so-called 1-min sustained winds is incorrect. Section 1.6 of HKG specifically advises on that topic noting that numerical models without explicit

eddy representation only estimate mean wind speeds, not gusts such as the so-called 1-min sustained wind. However, correcting for that (e.g. per HKG Table 1.2) will likely have no specific effect on the model performance.

Our numerically modeled winds are calculated on a timestep of a few seconds. This means that the model can only resolve wind variations of about 4 to 7 times the model timestep (depending on the variability of the flow). The instantaneous model outputs are therefore by no means the instantaneous wind. Rather, they are closer to the 1-minute average wind. It is true that our numerical modeling does not explicitly resolve turbulence. It parametrizes eddies. We agree with section 1.6 of HKG that the outputs of numerical models without explicit turbulence should be considered as the mean wind. And we consider the 1-minute wind to be a mean wind speed and not a gust measure. This is included on P9, lines 9-13.

(2.1) The authors state that the model is “agnostic to the source of the track data” as though that is some advantage, whereas the vast majority of historical datasets consist only of (lat, lon, Vmax) estimates with acknowledged high variability between agencies and also over-time. Rmax is also noted to be an essential parameter but is only recently available in some regions and not transparently derived. While these drawbacks are unavoidable, it further emphasises the challenge of using any (global) historical track data without critical assessment and expecting a high level of accuracy in the estimation of terrain-sensitive surface winds.

The cyclone-scale footprint will only be as good as the input best track data and the wind profile model. We also agree that details of how parameters such as Rmax are derived in historical track datasets are not transparent and are likely to vary wildly through time and between agencies. We have removed the statement that the model is “agnostic to the source of the track data” because while the model will function using different data sources, the accuracy of the cyclone-scale footprint will be very sensitive. This point has been made in the revised manuscript, P17, lines 2-4.

(2.2) While the Willoughby profile may be superior to some others for a hands-off global application it still requires an outer scale assumption and to note that TC scale, and its temporal evolution, is a critically important parameter in accurately modelling surface winds. The adopted land use surface roughness, with a scale of about 1 km, seems reasonable enough but should also be verified by example for the set of modelled storms. To note also that the references cited for drag coefficients are very dated and the authors could adopt more recent evidence to better suit their argued approach.

In response to this comment and a similar comment from another reviewer, Section 2.2 of the revised manuscript better highlights the assumptions needed to model the outer winds of the Willoughby profile. Firstly, we state that the length scale for the transition region across the eyewall is set to 25km when Rmax is greater than 20km and set to 15km otherwise. For the shape of the vortex outside Rmax, we hold the faster decay length scale fixed at 25km, following the recommendation of Willoughby et al. (2006), and allow the second length scale (XI) and the contribution of the fast decay rate (A) to vary the shape of the profile. For the slower decay length scale, we include note that Willoughby et al. (2006) show a wide range of the second length scale occurs in nature, with their Fig. 11 showing it can range from about 100 km to over 450 km. We therefore choose to allow A and XI to vary with the readily available parameters Rmax, Vmax and latitude, following Eqn. 11 in Willoughby et al. (2006).

The effects of the adopted land use surface roughness is included in the evaluation of the subset of U.S. storms shown in Fig. 4.

We have included an updated reference for the variation in surface drag over the ocean with wind speed. And we choose to keep the key early reference to Garratt (1977).

Comments on Results and Evaluation

(3.) The Puerto Rico example illustrates the intention and ability of the model to introduce terrain and topographic variability into its results but, without any verification, is otherwise meaningless and simply an "artist's impression".

We agree with the need to compare with available observations. This Puerto Rico example in Section 3 has been expanded (also in response to comments from other reviewers) to better demonstrate the effects of adding KW01, surface roughness, and topography. This expanded analysis also includes comparison with the available surface station data.

(4.) To note that the use of 3-h sampled wind data is typically inappropriate for TC passages within, say, 100 km and may be a principal source of the poor comparisons. Application of HKG Table 1.1 is also dubious given the 3-h sampling but more so because of its limited and nominal exposure classes, which appear inconsistent with the aim of deriving fine scale surface winds. HKG Section 1.2 says "The aim has been to provide a broad-brush guidance that will be most useful to the forecast environment rather than a detailed analytical methodology" and "In particular, post analysis of TC events should seek to use the highest possible site-specific analytical accuracy for estimating local wind speeds. This would include consideration of local surface roughness, exposure and topographic effects when undertaking quantitative assessments of storm impacts." This implies an approach like Powell et al. (1996) is needed in such cases. Again, these oversights in applying HKG will likely have little effect on model performance, but do point to a lack of rigour in matters of wind magnitude adjustment.

Thank you for this comment. We apologize that made a mistake in the text. In the original manuscript we incorrectly stated that "points are shown for all instances of the observed time falling within 3 hours of the model time." This didn't make sense, and has been corrected to "comparisons between observations and model are made using model time within 5 minutes of the observation time". We were able to do this because we output the model fields every 10 minutes.

We agree that the application of HKG Table 1.1 to scale the observations to the 1-minute wind is limited by the nominal exposure classes. But we also don't have the resources to conduct a detailed investigation into the specific exposure of each surface observing station. We therefore choose to leave this as an uncertainty in the evaluation. Over many surface observing sites over many landfalling events this uncertainty should approach zero if the effect is random. Though we agree that there is a clear need to conduct detailed site-specific comparisons in future work.

As noted previously, the demonstrated performance of the model is very poor compared with the numerous less-complex examples that are cited. In spite of the authors' tendency to downgrade the utility of H*WIND I would instead encourage pursuing such comparisons in order to locate the model deficiencies and improve its performance for the demonstration storms.

In our previous response we made the case that our approach is at least comparable to a recently published globally applicable model. It was not our intention to downgrade the utility of H*WIND. H*WIND has many benefits over our approach such as including the effects of storm-scale asymmetry unrelated to forward speed. Perhaps the only major disadvantage of H*WIND is that data are only available for a subset of U.S. storms.

One challenge of evaluating our model using H*WIND is the need for assumptions for how to convert our model wind speeds to the open terrain representation in H*WIND. While a comparison against H*WIND would be useful to explore the scales of variability that are not included in our modeling approach, we choose to restrict our evaluation to surface station data.

Comments on Global Landfalling TC Footprints

(5) The detailed commentary and interpretation of aspects of modelled landfall and inland wind decay characteristics in various localities seems to overlook the fact that the model is only reacting to the imposed “best track” intensity variation and therefore can have no better skill than offered by a simpler parametric approach. Surely fully dynamic modelling (e.g. HWRF or similar) is needed to reliably explore such impacts.

Our modeling approach only allows for one-way forcing by the gradient wind and pressure profiles on the tropical cyclone boundary layer. Possible upscale effects of local terrain back on the entire TC structure is not permitted and is therefore missed. For example, studies have shown that the TC track itself can be impacted by high mountain ranges (see the discussion in Ramsay and Leslie 2008). Our approach contains these effects to the extent they are contained in the input best track data. It is correct that our gradient winds are reacting to the imposed best track, but the winds at 10m above the ground are reacting to the local terrain. This separation of effects is more clearly stated in the revised manuscript. P17, lines 2-4.

We agree that NWP models would capture more of the terrain effects and therefore would be better suited to study terrain effects on the inland wind decay. But one of the goals of our study is to explore the effects across a global dataset, and generating this dataset would be computationally impractical for 2km resolution NWP modeling.

Modelling Global Tropical Cyclone Wind Footprints

James M. Done^{1,2}, Ming Ge¹, Greg J. Holland^{1,2}, Ioana Dima-West¹, Samuel Phibbs³, Geoffrey R. Saville³,
and Yuqing Wang⁴

- 5 ¹National Center for Atmospheric Research, 3090 Center Green Drive, Boulder CO 80301, US
²Willis Research Network, 51 Lime St, London, EC3M 7DQ, UK
³Willis Towers Watson, 51 Lime St, London, EC3M 7DQ, UK
⁴International Pacific Research Center and Department of Atmospheric Sciences, School of Ocean and Earth Science and
Technology, University of Hawaii at Manoa, HI 96822, US.
- 10 *Correspondence to:* James M. Done (done@ucar.edu)

Abstract. A novel approach to modelling the surface wind field of landfalling tropical cyclones (TCs) is presented. The modelling system simulates the evolution of the low-level wind fields of landfalling TCs, accounting for terrain effects. A two-step process models the gradient-level wind field using a parametric wind field model fitted to TC track data, then brings the winds down to the surface using a numerical boundary layer model. The physical wind response to variable surface drag and terrain height produces substantial local modifications to the smooth wind field provided by the parametric wind profile model. For a set of U.S. historical landfalling TCs the accuracy of the simulated footprints compare favourably with contemporary modelling approaches. The model is applicable from single event simulation to the generation of global catalogues. One application demonstrated here is the creation of a dataset of 714 global historical TC overland wind footprints. A preliminary analysis of this dataset shows regional variability in the inland wind speed decay rates and evidence of a strong influence of regional orography. This dataset can be used to advance our understanding of overland wind risk in regions of complex terrain and support wind risk assessments in regions of sparse historical data.

Deleted: full

Deleted: surface station observations.

1 Introduction

Tropical Cyclones (TCs) dominate U.S. weather and climate losses (Pielke Jr, et al., 2008; Smith and Katz, 2013). They account for 41% of the inflation-adjusted U.S. insured loss between 1995 and 2014. Future increases in TC peak wind speeds (Walsh et al., 2016), in combination with rapid population increases, mean TC wind losses are set to rise even further (Geiger et al., 2016; Estrada et al., 2015; Ranson et al., 2014; Weinkle et al., 2012). Improved approaches to assessing overland TC wind fields is needed to enable society to manage this increasing risk.

Deleted: .

While coastal communities may experience relatively frequent TC impacts, inland communities experience TC impacts far less often and less is known about the likelihood of inland damaging winds. Given the scientific consensus that average TC wind speeds will increase in the future (e.g., Villarini and Vecchi, 2013; Murakami et al., 2012; Hill and Lackmann, 2011; Elsner et al., 2008) and that category four and five hurricanes have increased substantially in recent decades (Holland and Bruyère, 2014), strong winds may be experienced farther inland in the future, all other TC and environment characteristics being equal. Modelling approaches that capture TC footprints - the entire overland swath of storm-lifetime maximum wind speed from the immediate coast to far inland - is therefore a key need.

Deleted: 4

Deleted: 5

Deleted: e

New views of global TC footprints are critically needed to support a variety of risk management activities. One particular need is to characterize overland footprints for mountainous countries that have both a high TC risk and significant insurance exposure, such as the Philippines and Japan. What is the impact of coastal terrain features on TC wind distributions and potential losses? And how does terrain affect overland extreme wind probabilities? In addition, a catalogue of global historical events may also be used to model losses from historical events. These scenarios stress-test reinsurance structures to ensure companies have adequate protection, and can also be used in submissions to regulators. Long records of TC overland wind

Deleted: techniques across a range of timescales

Deleted: At short timescales, in the immediate few days ahead of a landfalling TC, what is the physically credible range of footprint scenarios, and thus potential losses? At longer timescales,

Deleted: w

Deleted: Long records of TC overland wind footprints are also critically needed to appraise traditional modelling approaches, inform the generation of synthetic event sets (particularly in regions of sparse historical data), and to inform near- and long-term views of wind probability accounting for climate variability and incorporating the effects of climate change.

footprints also inform the generation of synthetic event sets (particularly in regions of sparse historical data), and inform near- and long-term views of wind probability accounting for climate variability and incorporating the effects of climate change. A global catalogue of TC wind footprints is also needed to advance our basic understanding of TC climate across basins. For example, what are the global- to local-scale processes controlling regional spatial and temporal trends and variability of overland TC winds?

Deleted: Historical event footprints can be used to better understand historical losses, and to create physically plausible worst-case TC scenarios, known as realistic disaster scenarios in the re/insurance industry.

Using an analytical boundary layer model to simulate the low-level winds during Hurricane Fabian (2003) over Bermuda, Miller et al. (2013) found winds at the crest of a ridgeline at category four strength compared to category two strength in simulations without terrain. Simulations of Cyclone Larry (2006) over the coastal ranges of Queensland, Australia using a full numerical weather prediction model by Ramsay and Leslie (2008) also produced wind speed-ups along hill crests and windward slopes. The high Froude number flow brought about by the high wind speeds and quasi-neutral stability causes flow directly over the terrain features with minimal lateral displacement. Under mass continuity, flow accelerates as the air column thins passing over higher terrain. This speed-up also supports wind-shear driven turbulence and enhances peak gusts. For high mountains, however, the wind has a greater potential to become blocked. While a neutral boundary layer is not guaranteed at large radii (e.g., Kepert (2012) indicates increasing static stability as subsidence increases at large radii) measurements of turbulent fluxes in high-wind environments between outer rain bands by Zhang et al. (2009) find shear production and dissipation to be the dominant source and sink terms of TKE.

Deleted: ,

Deleted: 4

Deleted: 2

Given that the work done by the wind in directly damaging structures varies by the cube of the wind speed (Emanuel, 2005), terrain effects on damage have the potential to be significant. Indeed, Miller et al. (2013) found that the greatest residential roof damage was located along the ridgeline and the windward slopes of Bermuda. Terrain effects were also found in residential wind damage patterns during Cyclone Larry in 2006 (Henderson et al., 2006) and during Hurricane Marilyn in 1995 across the Island of St Thomas in the Caribbean (Powell and Houston, 1998). Incorporating terrain effects could therefore improve wind risk assessments when compared to traditional analytic methods in regions of complex terrain, thus supporting potential losses assessments and underwriting decisions in re/insurance markets.

Deleted: Under mass continuity, the flow accelerates as the air column thins passing over higher terrain. This speed-up also supports wind-shear driven turbulence and enhances peak gusts.

Deleted: ,

Current practice in wind field modelling spans a range of complexity, depending on the application. The simplest models, known as parametric radial wind profiles fit functions to a small number of readily available TC and environmental parameters to characterize the radial profile of wind and pressure from the TC centre. The Holland et al. (2010) profile, for example, models the surface winds directly whereas the Willoughby et al. (2006) profile models the gradient-level winds and an extra step is needed to determine the surface winds. These models are computationally efficient and therefore widely used as the hazard component of catastrophe models (Mitchell-Wallace et al., 2017; Vickery et al., 2009), and can be used to compute wind exceedance probabilities anywhere on Earth. But fast computation comes at a price. The resulting wind fields are smooth, and so empirical corrections are typically applied to represent surface terrain effects.

Deleted: surface

Deleted: (e.g., Holland et al., 2010; Willoughby et al., 2006),

Deleted: surface

Deleted: y

An alternative approach is a reanalysis of observations. A reanalysis is created using a physical model that is nudged towards available observations. While a reanalysis produces gridded data and may capture observed asymmetries, it may still miss the effects of a variable surface roughness [e.g., HWIND (Powell et al., 1998) is representative only of open terrain], and to date only a small fraction of historical global events has been reanalysed. Another alternative approach is geostatistical spatial modelling. This data-driven approach combines spatial statistics to capture spatial dependence with extreme value theory to capture peak wind speeds. Again, this model is highly efficient but so far has only been developed for European windstorms (Youngman and Stephenson, 2016) to the authors' knowledge. Finally, four-dimensional high-resolution numerical modelling captures many more physical processes (e.g., Davis et al., 2010). But it is computationally too expensive and can be used only in a small number of cases. It is therefore of marginal use as the hazard component of catastrophe models, aside from use to develop improved parametric models (Loridan et al., 2015; Loridan et al., 2017).

This paper describes a novel and globally applicable approach to modelling the surface wind field of landfalling TCs. The model was developed as a collaboration between atmospheric scientists and reinsurance industry experts to ensure the model and resulting datasets are readily applicable to decision-making processes and based in peer-reviewed science. The modelling system combines the high efficiency of the parametric profile model with a representation of the interaction of the flow and variable surface terrain that captures the essential dynamics and physics. The modelling system simulates the temporal evolution of the near-surface spatial wind fields of landfalling TCs, accounting for terrain effects such as coastal hills and abrupt changes in surface roughness due to coastlines, forested or urban areas. The approach fits a parametric wind field model to historical or synthetic TC track data, and captures the frictional response of the wind field to the Earth's surface using a ~~three~~-dimensional numerical model of the lowest 2-3 km of the atmosphere.

Application of the model is demonstrated through the creation of a dataset of 714 historical landfalling TC footprints globally. Such global footprint datasets have been created before but none used a non-linear boundary layer model that captures the dynamical response to a variable lower boundary. Giuliani and Peduzzi (2011) utilized a dataset of global historical TC footprints generated using a parametric model. More recently, Tan and Fang (2018) generated a dataset of 5376 global historical footprints using an approach that simulates the gradient winds using a parametric wind profile model and bringing the winds down to the surface using a simple power law profile that depends on the local surface roughness (Meng et al., 1997). Terrain effects were included using a simple speed-up factor based on ~~four~~ categories of terrain type and wind direction. By using a ~~three~~-dimensional model our approach includes additional ~~physical terrain effects~~. ~~Our approach only considers the lowest 2-km of the atmosphere, thereby excluding the free troposphere needed for large-scale mountain waves to bring free-atmosphere winds down to the surface. It's also unlikely that our modelling approach has the resolution to capture flow-separation turbulence downwind of crests and escarpments. However, the physical terrain effects permitted by the model include convergence, vertical diffusion and vertical advection on windward slopes and crests resulting in locally strong low-~~

Deleted: 3

Deleted: 4

Deleted: 3

Deleted: dynamical

Deleted: such as non-linear development.

level shear and TKE production. In addition, the vertical boundary layer structure allows the potential for super-gradient jets (Franklin et al. 2003; Kepert and Wang 2001) to influence winds in high terrain. Finally, the time dimension allows for upwind effects due to upwind terrain variations and terrain to be incorporated.

5 The next section describes the modelling approach. Section 3 presents sensitivity simulations for a case study of Hurricane Maria (2017) over Puerto Rico to demonstrate the effects of adding the boundary layer model and variable terrain. A model evaluation against surface station observations is provided in Sect. 4. Section 5 describes the dataset of global historical landfalling TC footprints and includes a preliminary analysis. Finally, conclusions are presented in Sect. 6.

Deleted: de

Deleted: describes the simulation results of selected case studies.

Deleted: ion

Deleted: ion

2 Method

10 A TC footprint is generated using a two-stage modelling process bookended by pre- and post-processing steps, as summarized by the flow diagram in Fig. 1. Stage one fits a parametric model of upper winds and pressure to the input TC track data. Stage two applies a three-dimensional numerical boundary-layer model to generate a detailed surface wind field incorporating the effects of terrain features such as coastlines, inland orography, and variable land surface friction.

Deleted: 3

15 The pre-processing step removes an estimate of the asymmetry due to storm motion (V) from the maximum wind speed input from the TC track data. The extent to which asymmetry due to forward speed is included in best track wind speed is uncertain. But given that these winds are Earth-relative measurements we assume that removing an uncertain estimate of asymmetry produces a more accurate estimate of the rotational wind than the original best track wind speed. The portion removed is a function of the TC translation speed (V), $V=1.173V_{max}$, following Chavas et al. (2017). The post-processing step then adds back an estimate of the asymmetry due to storm motion to the output surface wind velocity field, again following Chavas et al. (2017). In addition, the fraction of this storm motion vector added is equal to one at the radius of maximum winds and then decays with increasing radius, following Jakobsen and Madsen (2004). Our approach therefore misses any interaction effects between terrain and the asymmetrical component of the storm wind field. The importance of these effects is unknown and we leave their inclusion for a future iteration of our model.

Deleted: ,

Deleted: T

Deleted: e

Deleted: l

25 The final footprint is a map of the storm lifetime maximum one-minute average wind at 10 meters above the Earth's surface. The boundary layer model of Kepert and Wang (2001, hereafter KW01) outputs the instantaneous wind speed at 10 meters above the surface which is the lowest model level. While the instantaneous wind field output from a numerical model does not directly correspond to a specific averaging interval, some guidance is provided by the model timestep. A typical KW01 timestep of four seconds adequately resolves variability at timescales of a minute. The footprint is then simply calculated as the storm lifetime maximum wind speed at each grid point. Frequent model output intervals or a weak smoother may be needed to minimize the appearance of rings of strong winds in the footprint, particularly for fast moving TCs.

Deleted: l

Deleted: -

Deleted: 4

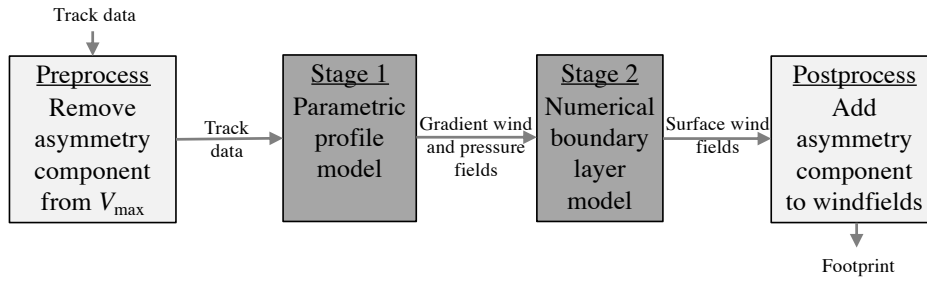


Figure 1: Workflow diagram of the two-stage modelling process, bookended by pre- and postprocessing steps.

5 2.1 Input Tropical Cyclone Track Data

The input TC track may be historical, synthetic or a real-time forecast. But the accuracy of the historical or forecast cyclone-scale footprints will be sensitive to the accuracy of the input track data. Typical historical data sources include the global International Best Track for Climate Stewardship (IBTrACS, Knapp et al., 2010), the Extended Best Track Dataset (Demuth et al., 2006, for the East Pacific and North Atlantic), or from the Joint Typhoon Warning Center (JTWC). Track data require latitude, longitude, maximum wind speed (V_{max}), radius of maximum wind (R_{max}), and environmental pressure. If the Holland et al. (2010) wind profile is used (discussed in the next section), an additional variable of the radius of 34 kt winds is required. Sensitivity tests (not shown) found that the model requires new track data every 10 minutes, to smooth out changes in the forcing of KW01 and reduce shocks. These can be obtained by simple interpolation.

Deleted: The model is agnostic to the source of the TC track data.

Deleted: To emphasize the use of only readily available data, we choose to use an average value of R_{max} around the storm.

Deleted: ,

Applying the modelling approach to create a dataset of global historical landfalling TC footprints requires as input the globally consistent IBTrACS v04 TC track dataset (Knapp et al., 2010). While Tan and Fang (2018) fill in missing variables using empirical relationships between TC variables, we choose to exclude tracks with missing data. For all basins, landfalling track points are identified using the landfall flag in the IBTrACS dataset (Knapp et al., 2010). Bypassing storms are included to capture the storms that don't make landfall, but still bring strong winds onshore. Such storms are identified using the 'distance to land' variable in IBTrACS, and defined as TCs that track within 50 km of a coastline, or within 250 km of the coastline with maximum wind speeds greater or equal to 50 kts (58 mph). Since our interest is in winds over land, storms are simulated

from approximately 12 hours before landfall (or before the closest point to land for bypassing storm) as far inland as the end of the track, or until the TC tracks back out over open water.

5 2.2 Stage 1: Modelling the Gradient-Level Wind and Pressure Fields

Initial solutions for the gradient-level spatial wind and pressure fields are created for each time step using a parametric profile model. The gradient-level solution represents upper winds unaffected by frictional and terrain effects from the lower surface boundary. One definition for the boundary layer height is the depth of the inflow, defined as the height where the radial inflow falls to 10 % of the peak inflow. Using radiosonde ascents in 13 hurricanes Zhang et al. (2011) find this height to be approximately 850 m at the radius of maximum wind rising to approximately 1300 m at larger radii. Parametric profile models use functional radial profiles to determine the wind speed and pressure field from the TC centre [see Vickery et al., (2009) for an overview]. Our modelling approach is flexibly adaptable to use most choices of radial profile model.

Sensitivity tests (not shown) with the Holland et al., (2010) and Willoughby et al., (2006) profiles showed some differences.

The Holland et al., (2010) profile has the advantage of tying down the radial decay profile using an observation of an outer wind, say the radius of 34 knot winds. However, observations of outer winds are not readily available globally. Willoughby et al., (2006) uses a sectionally continuous wind-profile comprising a power law inside the eye and two exponential decay functions outside. A polynomial smooths the transition across the radius of maximum wind. This allows greater flexibility for using those databases without 34 kt wind radii. The viability of forcing KW01 with the Willoughby profile was demonstrated by Ramsay et al., (2009) for a case study simulation of Tropical Cyclone Larry (2006), by Kepert (2006a) for

Hurricane Georges (1998), Kepert (2006b) for Hurricane Mitch (1998), and Schwendike and Kepert (2008) for Hurricanes Danielle (1998) and Isabel (2003). Willoughby et al., (2006) conducted a comprehensive evaluation using flight level data. The verified performance of Willoughby motivated our choice of Willoughby profile for all simulations presented in this paper.

The outer radius of damaging winds can be highly sensitive to the choice of free parameters. The length scale for the transition region across the eyewall is set to 25km when R_m is greater than 20km and is set to 15km otherwise. For the shape of the vortex outside R_m , we hold the faster decay length scale fixed at 25km, following the recommendation of Willoughby et al. (2006), and allow the second length scale (X_1) and the contribution of the fast decay rate (A) to vary the shape of the profile. Willoughby et al. (2006) showed a wide range of the slower decay length scale occurs in nature, from 100 km to over 450 km. Given that aircraft data are not uniformly available globally and our intention to only use readily available data (and the difficulties in using aircraft reconnaissance data as discussed in Kepert 2006a,b and Schwendike and Kepert 2008), we decide not to include these additional data sources for subsets of global historical events. Willoughby et

Deleted: For TCs this level is typically between 500m and 1.5km above the surface, depending on definition, and decreasing towards the TC centre (Zhang et al., 2011).

Deleted: .

Deleted: .

Deleted: .

Deleted: .

Deleted: .

Deleted: .

Deleted: fewer required data inputs and the

Deleted: We choose to calculate profile parameters using Eqn. (11) of Willoughby et al., (2006) to capture dependencies on R_m .

al. (2006) demonstrated dependence on V_m and latitude, with the more intense low latitude TCs being more sharply peaked. We therefore choose to allow the remaining two free parameters (A and $X1$) to vary with readily available parameters R_m , V_m and latitude, following equation 11 in Willoughby et al. (2006). This globally consistent approach is needed to allow relative risk assessments across regions.

5 The Willoughby profile requires V_m at gradient wind level. The input track V_m is almost universally an estimate of the surface value, so an inflation factor is used to inflate the wind estimate from a surface to a gradient level value. Franklin et al. (2003) observed an inner core wind maximum at about 500m that increases to about 1km for the outer winds. They found a logarithmic profile below the wind maximum and a reduction of winds above due to the warm core. The result is a 700-hPa-to-surface wind factor of about 0.9 in the inner core. Kepert and Wang (2001) theory also has a factor of 0.9 in the inner core, with the factor decreasing to 0.75 in the outer winds. Knaff et al. (2011) took the Franklin et al. (2003) factor of 0.9 in the inner core and additionally reduced it by a factor of 0.8 to go from marine-exposure winds to terrestrial-exposure winds, giving a net factor of $0.9 \times 0.8 = 0.72$. Initial testing using a variable factor for offshore and onshore track caused enhanced winds just offshore in response to the higher factor for the first inland track point. This is because the outer winds were still responding to the low surface roughness while being driven by stronger gradient winds. We therefore choose to hold the factor fixed at 0.76 (also based on sensitivity testing, not shown) and appropriate for inland winds.

Deleted: of 1.32

Deleted: While this represents a tunable parameter in our approach, it was selected based on our sensitivity tests for a few historical events (not shown). These sensitivity tests showed KW01 produced inflation factors for surface-to-gradient level wind speeds ranging from 1.11 to 1.43 around the vortex, which agree well with the mean value of 1.32 obtained from 150 dropsonde observations by Powell et al., (2003).

2.3 Stage 2: Modelling the Atmospheric Boundary Layer

A key advance of our modelling approach over traditional approaches is the use of a numerical boundary layer model to generate a surface wind field. Winds in the boundary layer, the layer between the gradient wind level and the surface, are modelled using a modified version of KW01. KW01 is initialized with the gradient-level wind and pressure fields from the parametric model throughout the entire depth of the boundary layer. It then uses the dry hydrostatic primitive equations (solving for atmospheric flow under conservation of mass, conservation of momentum and accounting for heat sources and sinks) to spin up a steady state boundary layer wind structure in balance with the gradient winds and pressures. Moisture is excluded from the model because of its negligible effects on boundary layer flow. We selected this non-linear model because of its ability to develop important boundary layer structures such as the super-gradient jet (KW01; Kepert, 2006).

Deleted: ntag

The model rapidly achieves steady state in the strongly forced TC environment characterized by large momentum fluxes and fast adjustments (not shown). The model has 18 vertical levels on a height-based vertical coordinate with the model top fixed at 2.0km. This height was chosen to be above the height of super-gradient jets, and to be above the typical range of the radially-dependent boundary layer top (Kepert et al. 2012). This number of vertical levels is far higher than used in most numerical weather prediction models. While the boundary layer height likely varies substantially across global TCs, we choose to keep

this fixed in the absence of readily available data. Sensitivity tests (not shown) show that horizontal grid spacings of 2 to 4 km are sufficient to maintain the tight pressure gradients of strong TCs, and to capture the effects of major terrain features such as coastal ranges or coastal urban areas.

Deleted: -

5 The highly turbulent boundary-layer flow is treated using a high order turbulence scheme with prognostic turbulent kinetic energy and turbulence dissipation, following Galperin et al. (1988). The turbulence length scale is diagnostic and is capped at 80 m following Blackadar (1962). While the model parameterizes shear-driven turbulence, it does not well represent strong thermal effects such as buoyancy. But these thermal effects are negligible for most TC boundary layers where the Richardson number (the ratio of buoyancy-driven to shear-driven turbulence) is close to zero. Harper et al. (2010) state that the outputs of numerical models without explicit turbulence should be considered to be the mean wind. Our numerically modelled winds are calculated on a timestep of a few seconds. The model can therefore only resolve wind variations of about 4 to 7 times the model timestep, depending on variability of the flow. The instantaneous model outputs are therefore not the instantaneous wind, but closer to the 1-minute mean wind.

Deleted: ,

Deleted: ,

Deleted: captures the effects of

15 The original model coordinates of KW01 are storm-relative. Here, model coordinates are changed to Earth-relative. Each simulation is conducted on one of the 17 geographically-fixed regional domains, shown later in Fig. 5. For the simulation of an entire storm footprint, the forcing of the model from the upper winds and pressure field is updated every 10 minutes. While KW01 found 24 hours was needed for the boundary layer to spin up an equilibrium state, running for 24 hours for each forcing update is computationally impractical. Sensitivity tests (not shown) showed that the surface winds, the most important for this study, respond rapidly to changes in the forcing.

Deleted: ;

Two code modifications were necessary for the simulation of time-evolving and landfalling TCs. The first allows the boundary layer solution to respond to translating TCs and TCs that change in intensity and/or size. The upper winds and pressure are fixed to the parametric model at each time step, to force the boundary layer winds to keep up with the translating storm. In addition, a translation vector is added to the horizontal advection terms in KW01. The portion of the translation vector added reduces close to the surface due to surface friction. To allow the boundary layer winds to respond to changes in vortex structure, the forcing of the model from the upper winds and pressure field is updated every 10 minutes and interpolated to each time step.

Deleted: In addition, the boundary layer solution has a memory through the translating advection terms.

Deleted: The second

Deleted: 3

25 A code modification allows the boundary layer solution to respond to real-world terrain height and surface roughness as the TC tracks over land. Terrain elevation data are provided by the Global Multi-Resolution Terrain Elevation Dataset 2010 at 30 arc-seconds (Danielson and Gesch, 2011), and are interpolated onto the model grid. Terrain height enters the boundary layer model through the computation of vertical diffusion and vertical advection, where higher terrain enhances both. Terrain height is first normalized by the height of the model top and capped at 0.9. Vertical motion is diagnosed through the three-dimensional continuity equation integrating upwards given terrain height and horizontal velocity. Mass may therefore enter or exit the model top according to the requirement to balance net horizontal convergence. Land-use roughness is provided by the MODIS-based 21 category land use data at 30 arc-seconds. The model feels the variable surface roughness through the drag coefficient term.

30 Over land a neutral drag coefficient depends on the surface roughness (Garraff, 1977). Over the ocean, the Charnock relation modified by Smith (1988) is used to account for the effects of increased roughness as wave heights grow with wind speed (see also Powell et al., 2003).

Deleted: e

3 Case Study: Hurricane Maria (2017)

A series of simulations of increasing model complexity is presented here to illustrate the importance of variable land surface friction and terrain height. Using the case study of Hurricane Maria (2017) over Puerto Rico we first compare simulations using the Willoughby profile only, and the addition of KW01. All simulations were run at 2 km grid spacing. The Willoughby profile (Fig. 2a) places the strongest winds to the right of track, as expected. It captures the decaying winds as Maria crosses Puerto Rico but it misses any abrupt changes in the onshore and offshore flow, also as expected. In the absence of changing surface friction and terrain at landfall, the only information the model has about landfall is through the decreasing V_m in the input track data. The addition of the boundary layer model (KW01, Fig. 2b) brings an overall reduction of the footprint (compare Figs. 2a and 2b) and much greater small-scale variability in the footprint over land. Variable terrain height results in wind acceleration over elevated terrain. Variable surface roughness results in sharp transitions in the wind speed along coastlines and, for example, over the urban area of San Juan in the northeast of mainland Puerto Rico. The winds weaken abruptly as Maria makes landfall and the boundary layer model adjusts to the increased surface friction of the land surface. Maximum values of the footprint in the vicinity of the track agree reasonably well with the input track V_m values (shown by the coloured dots along the track). The surface reduction factor (the ratio of Fig. 2a and Fig. 2b), shows strong spatial variability (Fig. 2c). The reduction factor ranges between 0.5 and close to 1.0 according to the spatial surface roughness and spatial terrain height.

A snapshot of the simulation using the Willoughby profile and KW01 at the time of landfall is shown in Fig. 2d. Onshore winds decay over land in response to the enhanced surface roughness, overland winds accelerate over elevated terrain, and offshore winds accelerate over the water. Interestingly, wind vectors suggest the high momentum air is carried directly over local terrain features with no evidence of flow deviations or blocking (upstream deceleration).

A scatter plot of model (using the Willoughby profile and KW01) versus observed 1-minute wind speeds throughout the lifetime of the storm at the locations of surface observing stations is shown in Fig. 2e. Observations are provided by the 3-hourly NMC ADP Global Surface Observations Subsets (NCEP/NWS/NOAA/U.S. Department of Commerce). Wind averaging periods are converted from two-minute to one-minute for onshore station data and from 10-minute to one-minute for offshore buoy using the World Meteorological Organization conversion factors in Table 1.1 of Harper et al. (2010). Comparisons between observations and model are made using model time within 5 minutes of the observation time. We choose not to adjust for the complex exposure differences across the observing sites or between the observing sites and the model exposure representation.

Differences between model and observations are mostly within $\pm 10 \text{ ms}^{-1}$ across Puerto Rico (Fig. 2e). While a perfect correspondence between model and observations would lie along the one-to-one line, some scatter is expected due to the

Deleted: Results

Deleted: ly

Deleted: orography

Deleted: i)

Deleted: ii)

Deleted: Willoughby profile and

Deleted: but without land

Deleted: , and iii) the Willoughby profile and KW01 with land.

Deleted: Figure 2 compares the three footprints.

Deleted: Figure 2a shows that the Willoughby profile

Deleted: d

Deleted: b

Deleted: by approximately 10% as KW01 responds to the effects of surface friction of the sea surface, as expected. Maximum values of the footprint in the vicinity of the track agree well with the input track V_m values (shown by the coloured dots along the track). Finally, the addition of land including variable surface roughness and terrain height (Fig. 2c) causes much greater small-scale variability in the footprint over land. Variable terrain height results in wind acceleration on windward slopes and mountain crests. Variable surface roughness results in sharp transitions in the wind speed along coastlines and, for example, over the urban area of San Juan in the northeast of mainland Puerto Rico.

relatively coarse model grid not resolving fine-scale variability and the loss in predictability of fine-scale variability. While there is evidence of a small high wind speed bias, particularly for low wind speeds, we choose not to tune the model to a single storm. An evaluation over a collection of storms is presented in the next Section.

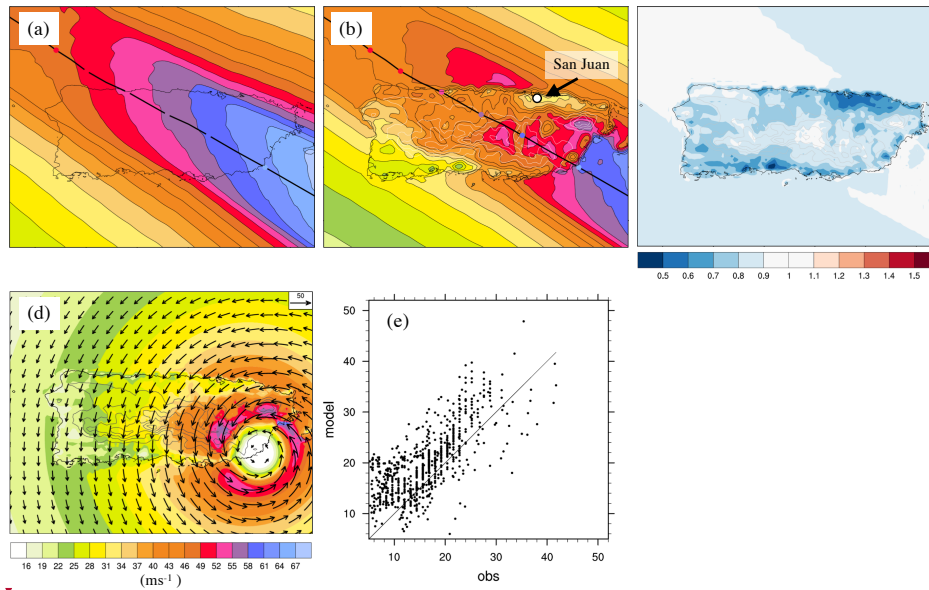
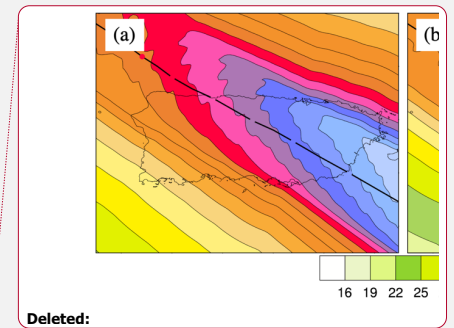


Figure 2: Case study simulation of Hurricane Maria (2017) over Puerto Rico. Simulated footprints (ms⁻¹) are shown using (a) Willoughby only, (b) Willoughby and KW01. The hurricane track is shown by the thick black line with input V_{in} shown every six hours along the track (coloured dots). Coastlines are shown by the thin black lines, and are only included in (a) to aid interpretation. (c) The ratio of Willoughby and KW01 to Willoughby only. (d) A snapshot of the simulation using Willoughby and KW01 at the time of landfall (wind speed is contoured and wind vectors are shown in arrows). Terrain height is contoured every 200 m in (b) – (d). (e) A comparison of observed and simulated (Willoughby and KW01) winds.

The effects of variable surface roughness and terrain height are explored in detail through a series of sensitivity simulations, again using the case of Hurricane Maria (2017) over Puerto Rico. These sensitivity simulations all use the Willoughby profile and KW01 but differ in the representation of the land surface. The representations are i) no land (entire domain set to water, referred to as NO LAND) to isolate the effect of adding KW01 to Willoughby, ii) no terrain height (entire domain is flat,



Deleted:

Deleted: for the case of Hurricane Maria (2017) over Puerto Rico using a) Willoughby only, b) Willoughby and KW01 and no land, and c) Willoughby and KW01 including land

Deleted: 6

Deleted: and b)

Deleted: Terrain height is contoured every 200m using white lines in c).

referred to as NO_OROG) to isolate the effect of adding variable surface roughness, and iii) all surface roughness set to open water values but retaining terrain height (referred to as NO_ROUGHNESS) to isolate the effect of variable terrain height.

5 NO LAND (shown in Fig. 3a) shows a spatially smooth reduction in wind speeds compared to the simulation using the Willoughby profile only (compare with Fig. 2a). The reduction factor is approximately 0.9 (Fig. 3d). NO_OROG (Fig. 3b) shows the strong frictional effect of the drag of the land surface on the boundary layer winds. The wind reduction factor (relative to NO LAND) falls below 0.6 over the roughest terrain (the variable roughness is shown in Fig. 3g). Finally, NO_ROUGHNESS shows wind acceleration over elevated terrain (see Figs. 3c and 3f). The wind enhancement factor (relative to NO LAND) increases with terrain elevation but does not exceed 1.3 across Puerto Rico.

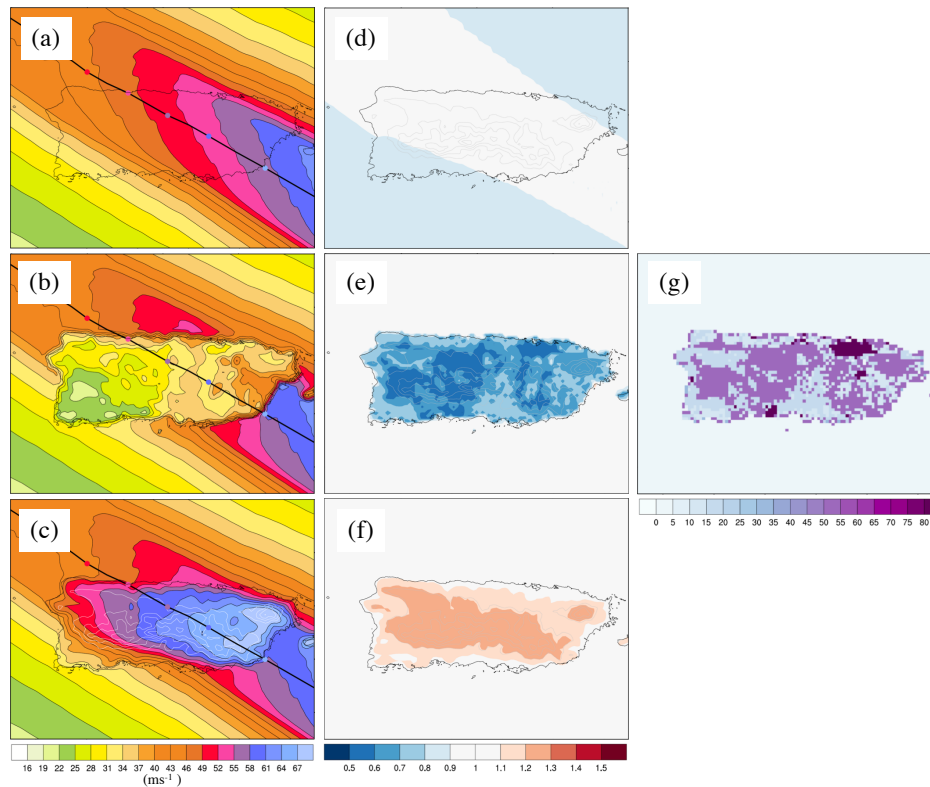


Figure 3: (a) – (c) Simulated footprints (ms) of Hurricane Maria (2017) over Puerto Rico using Willoughby and KW01 with (a) no land (NO LAND), (b) no terrain height (NO OROG), and (c) constant surface roughness equal to the ocean value (NO ROUGHNESS). The hurricane track is shown by the thick black line with input V_m shown every six hours along the track (coloured dots). Coastlines are shown by the thin black lines, and are only included in (a) to aid interpretation. (d) Ratio of Willoughby only to NO LAND. (e) Ratio of NO LAND to NO OROG. (f) Ratio of NO LAND to NO ROUGHNESS. (g) Surface roughness (cm).

4 Evaluation

Keprt (2012) notes that “The boundary layer in a tropical cyclone is in some respects unlike that elsewhere in the atmosphere. It is therefore necessary to evaluate boundary layer parameterizations for their suitability for use in tropical cyclone simulation.” Here we present a model evaluation for a subset of historical landfalling TCs to assess the model’s capability to reproduce observed surface wind speeds.

While reanalysis products provide historical footprints as a convenient gridded product, they themselves are a modelled product that contains various assumptions and inaccuracies. In addition, reanalyses are typically standardised to a given land surface type. The HWIND reanalysis product (Powell et al., 1998), for example, is only valid for open-terrain exposure and therefore commonly exceeds wind values from surface observing stations. We therefore choose to evaluate the model against the surface station observations provided by the 3-hourly NMC ADP Global Surface Observations Subsets (NCEP/NWS/NOAA/U.S. Department of Commerce). Since the U.S. has the highest density observing sites, a subset of eight U.S. landfalling storms was chosen for the evaluation. This subset includes storms making landfall on the Gulf Coast (Rita (2005), Katrina (2005) and Ivan (2004)), Florida (Charley (2004), Irma (2017) and Wilma (2005)), and the U.S. Northeast (Sandy (2012) and Irene (2011)).

Model performance across the eight U.S. storms is summarized in Fig. 4. To better understand model performance, the comparison with observations explores model bias as a function of distance from the TC centre, and split by left-of-track and right-of-track. Comparisons between observations and model are made using model time within 5 minutes of the observation time. Figures 4a and 4b show there is little evidence of large bias with the vast majority of differences falling within ± 10 ms. There is also no strong variation in bias with distance from the storm centre. A possible explanation for an apparent low bias within 20 km of the storm centre is storm centre location error in the input track data. Our approach compares favourably with a recently-published global modelling approach. The approach of Tan and Fang (2018) that combines parametric wind profile modelling with local wind multiplication factors produces typical errors of 8 to 10ms in the 10-minute mean wind. In addition, this magnitude error can also be present in hurricane surface wind vectors utilizing C-band dual-polarization synthetic aperture radar observations, when compared to collocated QuikSCAT-measured wind speeds (Zhang et al. 2014).

Deleted: .

Deleted: .

Deleted: Wind averaging periods were converted from 2-minute to 1-minute for onshore station data and from 10-minute to 1-minute for offshore buoy using the World Meteorological Organization conversion factors in Table 1.1 of Harper et al., (2010).¹

Deleted: 8

Deleted: An example model comparison with observations is shown in Fig. 3 for Hurricane Wilma in Florida. For risk management the accuracy of wind speeds over urban is of critical importance. For the model to be as useful as possible a low wind speed bias over urban areas is corrected in a post-processing step. A bias correction factor of 20% is applied to the wind speeds over urban areas. This factor was determined through the evaluation of the full subset of storms described later in this section. The effect of this correction can be seen over the urban area of Miami for the case of Hurricane Wilma in Fig. 3a¹

Figure 3a shows the simulated footprint places the strongest winds to the right of track for this fast-moving storm, as expected. The winds weaken abruptly as Wilma makes landfall and the boundary layer model adjusts to the increased surface friction of the land surface. The lack of significant topography over South Florida allows the effect of variable overland surface roughness to be seen. The largest perturbation is the acceleration over the low friction surface of Lake Okeechobee. Finally, the footprint shows the reacceleration of winds as Wilma exits Florida, due to the increasing intensity of Willoughby’s gradient wind profile and the reduced surface friction. The strongest footprint winds compare well to the input track winds (compare the coloured contours with the coloured dots along the track line in Fig. 3a). The spatial footprint compares well with the reanalysed HWIND footprint (http://www.hwind.co/legacy_data/, Powell et al., 1998) (compare Figs. 3a and 3b). Both footprints capture similar overland wind speeds and asymmetry. But the footprint captures more small-scale variability such as the over-lake wind speed-up not permitted by the open-terrain exposure assumption of HWIND.¹

Deleted: A comparison of the storm lifetime maximum wind speed at the locations of available surface station observations is shown in Fig 3c. Differences between model and observations are mostly within ± 8 m/s across Florida. The same comparison between HWIND and surface station observations is not shown because the adjustment to open-terrain exposure in HWIND means the observations are not comparable. Figure 3d shows a scatter plot of¹

Deleted: 8

Deleted: Again, points are shown for all instances of the observed time falling within 3 hours of the model time.

Deleted: m/s

Deleted: P

Deleted: s

Deleted: are i)

Deleted: .

Deleted: or ii) use of an average value for Rmax. Our use of this average value was to enable use of readily available data. A next¹ [2]

The model performs similarly well on both sides of the storm, indicating that our treatment of asymmetry due to translation speed captures a major portion of the observed asymmetry. Figures 4c and 4d show only urban locations that observed winds exceeding 18 ms⁻¹. While there is a suggestion of a low bias for winds far from the storm centre, the vast majority of points lie within 10 ms⁻¹ of the observations. The most damaging winds also reside close to R_{max} (in the range 20-100 km from the TC centre) where our bias is smallest. Holmes (2007) found that the roughness length for urban areas can vary between 0.1 and 0.5 m for suburban regions and rise to between 1 and 5 m for densely packed high-rises in urban centres. Our model uses a single roughness length for all urban areas (suburban and city centres) of 0.8m, taken from the MODIS land use dataset. This value may be too high for suburban areas, where a value closer to 0.2 is typical (Yang et al. 2014). Depending on the specific siting of the wind observing stations, it's probable that the introduction of multiple urban categories with different roughness lengths would improve our low wind speed bias.

Deleted: Considering

Deleted: experienced

Deleted: (Figs. 4c and 4d), after applying the 20% bias correction factor the model shows no large bias

Deleted: .

Deleted: -

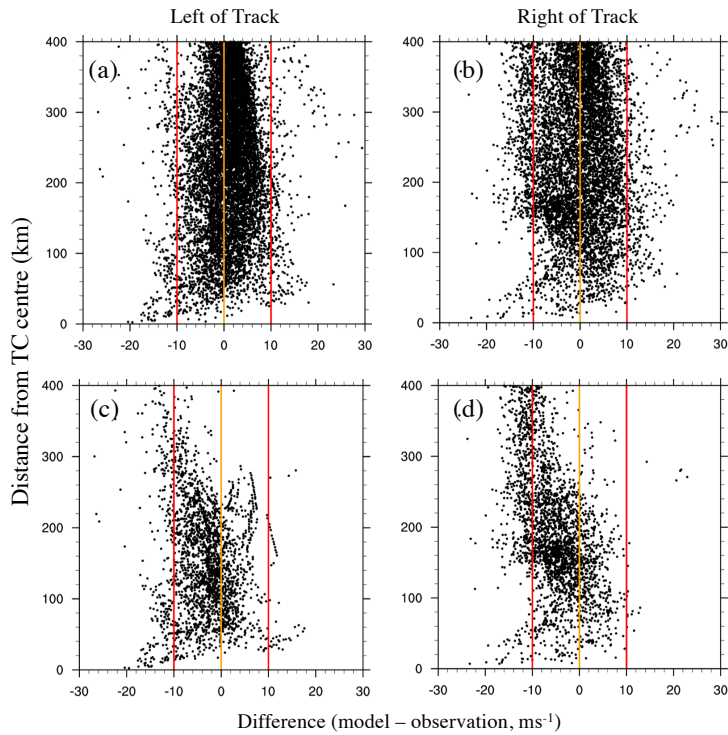
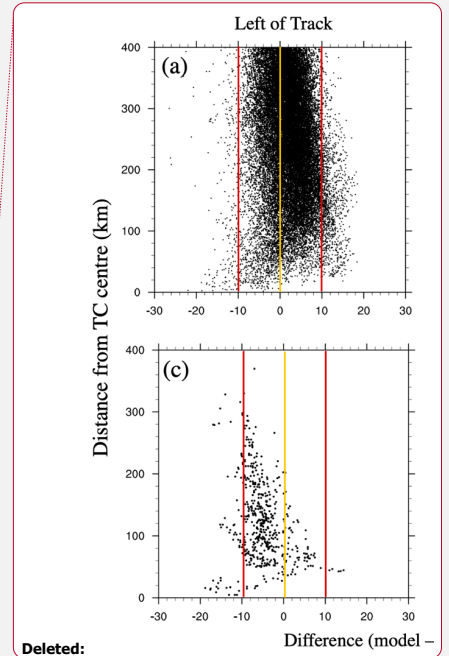


Figure 4: Difference between modelled and observed wind speeds for the 8 U.S. storms as a function of distance from the TC centre (ms^{-1}) and split by left of track (left column) and right of track (right column). The upper row shows all data points, and the lower row shows only urban data points that experienced observed wind speeds greater than 18 ms^{-1} . The orange lines indicate zero difference and the red lines indicate a positive and negative difference of 10 ms^{-1} .

5. A Dataset of Global Historical Landfalling TC Footprints

One application of the model is demonstrated here through the creation of the dataset of global historical landfalling TC footprints. The dataset consists of 714 footprints. Figure 5 shows the locations of 17 simulation domains together with the numbers of simulated footprints per domain. Figure 6 shows all tracks simulated for three example domains: The Gulf and Southeast U.S. coast, Eastern China and Taiwan, and Eastern Australia. The numbers and spatial density of tracks vary due to



Deleted:

Deleted: For global consistency, the input track data source is the global IBTrACS v04 dataset (Knapp et al., 2010). The data record length extends as far back as the required input data are available. Archived R_{in} data extend back to 1988 for the North Atlantic and the East Pacific, but extend back only as far as the early 2000s for the other basins. While Tan and Fang (2018) fill in missing variables using empirical relationships between TC variables, we choose to exclude tracks with missing data. For all basins, landfalling track points are identified using the landfall flag in the IBTrACS dataset (Knapp et al. 2010). Bypassing storms are included to capture the storms that don't make landfall, but still bring strong winds onshore. Such storms are identified using the 'distance to land' variable in IBTrACS, and defined as TCs that track within 50km of a coastline, or within 250km of the coastline with maximum wind speeds greater or equal to 50kts (58mph). Since our interest is in winds over land, storms are simulated from approximately 12 hours before landfall (or before the closest point to land for bypassing storm) as far inland as the end of the track, or until the TC tracks back out over open water.

Deleted: final

different periods of records for the different basins and the different frequencies of landfalling storms. Each footprint contains the storm lifetime maximum 1-minute average wind at each grid point at 10 meters above Earth's surface. The units are meters per second. Each footprint is on a latitude longitude grid with a grid spacing between 2 and 4 km depending on the regional domain.

Deleted: -
Deleted: -

5

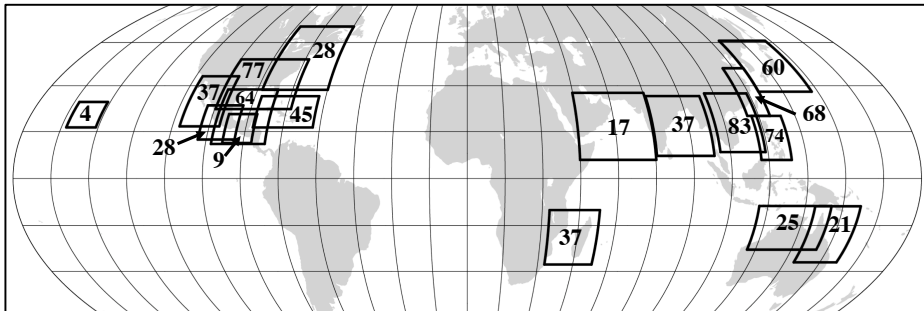


Figure 5: A global map of the 17 simulation domains used in the creation of the dataset of historical global TC footprints. The data record length extends as far back as the required input data are available. Archived R_{ms} data extend back to 1988 for the North Atlantic and the East Pacific, but extend back only as far as the early 2000s for the other basins. The numbers of simulated footprints for each domain is indicated.

10

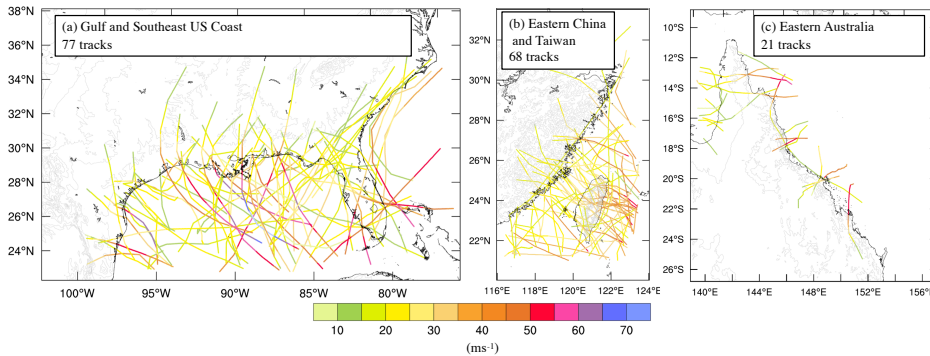


Figure 6: TC tracks used to simulate footprints for domains over a) the Gulf and Southeast U.S. coast, b) Eastern China and Taiwan, and c) Eastern Australia. Tracks are coloured by the track V_{max} (ms^{-1}). Track data are taken from IBTrACS (Knapp et al. 2010).

15

Tan and Fang (2018) suggest substantial regional variations exist in the inland extent of strong wind. A preliminary analysis of regional variability in the wind speed decay rates with inland track distance is presented here. Given that the simulated gradient winds are driven by the input best track data, the cyclone-scale inland decay is included to the extent it is included in the best track data. Additional sub-cyclone-scale terrain effects are included through the interaction of KW01 and the surface.

5 Figure 7 shows the regional average along-track distance rate-of-change of storm lifetime maximum wind speed and terrain height with along-track distance from the point of landfall for the Gulf and Southeast U.S. coast, Eastern China and Taiwan, and Eastern Australia (the same regions as shown in Fig. 6). The wind data are extracted from each wind swath at the location of the TC track. This data is therefore the storm lifetime maximum wind speed at specific locations along each TC track. All along-track wind data for a given region are then composited about their points of landfall, giving the region-average along-
10 track wind swath vs. distance inland. All data are additionally smoothed using a 30 km running average. The strength of the smoother was chosen as a balance between the need to smooth noisy wind profiles while retaining the effects of coastlines and terrain. The x-axes (along-track extent) extend until the distance inland at which only three tracks remain.

For the Gulf and Southeast U.S. region averages are calculated over 77 tracks. We see two regimes of behaviour (Fig. 7a). The
15 winds strongly decay at the coast as the boundary layer adjusts to the increased surface roughness. The winds then decay more moderately as the tracks extend further inland. The average along-track terrain gradient gradually rises to a peak of 210 m at an along-track distance of 550 km from the point of landfall and does not appear to substantially affect the inland wind profile. For other regions, however, steeper orography appears to have a large effect on the inland winds.

20 Figure 7b shows the average along-track winds calculated over 68 tracks over Eastern China and Taiwan. The average landfall wind speed of 29 ms⁻¹ experiences an abrupt decay at the immediate coast, followed by a modest recovery as the storms pass over the steep windward slopes of Taiwan and mainland China. The winds then experience some of the strongest decay rates in the entire dataset on the lee-side. The distance rate-of-change of wind speed is the net effect of orography, surface roughness and the overall inland decay according to the input best track data. This makes it challenging to isolate the processes driving
25 the inland wind speed gradient. It's possible that the increasing along-track terrain height drives enhanced vertical diffusion and vertical advection in the boundary layer model, and enhanced horizontal flow through the three-dimensional continuity equation. But idealized modelling would be needed to identify the presence and strength of this proposed mechanism.

30 The strong influence of terrain is also seen along the coastal ranges of Eastern Australia. Figure 7c shows three peaks of between 250 m and 280 m in the average terrain height along 21 tracks within 300 km of the average point of landfall. Again, the average landfall wind speed of 28 ms⁻¹ experiences a strong wind decay at the immediate coast before recovering slightly over the first ridgeline and then strongly decaying on the lee side. The rate of decay lessens over the second and third ridgelines. Overall, the relationship between wind change and terrain height does not appear to exhibit lead-lag behaviour.

Deleted: Region average values are calculated over all tracks within each region and

Deleted: a

Deleted: -

Deleted: are cut off

Deleted: at

Deleted: when

Deleted: 1

Deleted: 3

Deleted: The winds then experience some of the strongest decay rates in the entire dataset on the lee-side.

This preliminary analysis suggests a strong influence of regional terrain on overland footprints. Further investigation is needed to better quantify the effect and understand the extent to which the full range of terrain effects on TC wind fields are captured by this modelling approach.

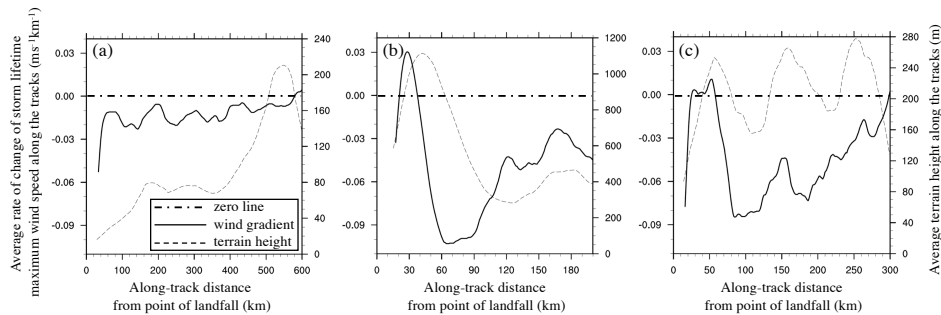


Figure 7: Variation of regional average distance rate-of-change of wind speed ($\text{ms}^{-1} \text{km}^{-1}$) and terrain height (m) with along-track distance from the point of landfall (km) for the same regions as shown in Fig. 6; a) Gulf and Southeast U.S. coast, b) Eastern China and Taiwan, and c) Eastern Australia. All data are smoothed using a 30 point running average. Region average values are calculated over all tracks within each region. The x-axes (along-track distance) are cut off at the point where only three tracks remain. Each panel has the same left y-axis limits but different right y-axis limits to better show the ranges of regional terrain height.

6. Conclusions

This paper presented a novel and globally-applicable approach to modelling the surface wind field of landfalling TCs. The modelling system simulates the temporal evolution of the near-surface spatial wind fields of landfalling TCs, accounting for terrain effects such as coastlines, inland orography, and abrupt changes in surface friction. A two-step process models the upper wind field using a parametric wind field model fitted to TC track data, then brings the winds down to the surface using a numerical boundary layer model. This represents more of the boundary layer physics and physical terrain effects than analytical approaches or empirical wind reduction factors. The guiding principles for model development were to i) use only readily available track data from historical archives, real-time forecasts or synthetic track models, and ii) maintain balance between representing the necessary physics of the land surface-flow interactions and the need for computational speed for future applications to probabilistic wind speed assessment.

The model is suitable for simulating the near-surface wind field throughout the entire lifecycle of translating, strengthening/weakening, expanding/contracting, and landfalling TCs.

Deleted: -

Deleted: 3

Deleted: dynamics and physics of the boundary layer

Deleted: , especially over regions of complex terrain

An evaluation of a subset of eight U.S. landfalling TCs against surface station observations showed that the model had no large bias across all storm radii, and across both sides of the storm tracks.

Deleted: 8

Deleted: This suggests that the treatment of asymmetry (the addition of a radially-varying fraction of the TC translation vector) captures much of the observed asymmetry.

For a case study of Hurricane Maria (2017), the inclusion of variable surface friction and terrain height was shown to add substantial sub-storm scale variability to the footprint. Winds dropped abruptly at the coast, yet accelerated over windward slopes and mountain crests. Winds also decelerated over the high surface drag of urban areas. The gradient-level to 10-meter reduction factor ranged between 0.5 and close to 1.0 according to the spatial surface roughness and spatial terrain height. Separating the surface roughness and terrain height effects showed surface roughness factors can fall below 0.6 whereas terrain height enhancement factors did not exceed 1.3. Analysis of wind vectors suggest that high momentum air is carried directly over local terrain features with no evidence of flow deviations or local blocking. Our modelling approach does not allow any blocking to affect the TC track itself, although the observed track data do include such blocking effects.

Further work is needed to verify the extent to which the full terrain and surface drag effects are included in the modelling approach. In addition to a process-level evaluation against observations, the efficacy of the approach could be assessed through comparison with numerical weather prediction (NWP) model simulations to understand where the approach fails. But differences in observed and NWP simulated TC tracks would need careful consideration. The overarching aim would be to identify the key terrain effects needed to be included in computationally efficient overland TC wind models.

Deleted: and vertical model grid spacings

An evaluation of a subset of eight U.S. landfalling TCs against surface station observations showed that the model had no large bias across all storm radii, and across both sides of the storm tracks. Our approach compares favourably with a recently-published global modelling approach and differences between different observing systems. Considering only urban locations that had observed winds greater than 18 ms⁻¹ there is a suggestion of a low bias. This may be due to our use of a single urban roughness length of 0.8m that is high compared to other studies.

The challenge of developing a globally applicable approach is that the accuracy at the individual event level will be lower than for a model developed for individual events or specific regions. We therefore do not expect our approach to improve upon individual event-level approaches that assimilate additional observational data. But a globally applicable approach has a number of unique benefits that derive from its small amount of required input data and physical response of the boundary layer winds to terrain. These benefits include generating events in data sparse-regions, generating synthetic events, and application to downscaling TC tracks from global climate models

An application of the model was demonstrated through the creation of a dataset of 714 global historical TC footprints, and is referred to as the Willis Research Network Global Tropical Cyclone Wind Footprint dataset version 1. While previous studies have mapped global historical TC wind fields, none included the nonlinear adjustments of the surface wind field to variable

Deleted: full

terrain. This unique dataset is a rich resource to advance our process-level understanding of spatial and temporal variability in overland TC winds. A preliminary analysis showed strong regional variability in the inland extent of damaging surface winds, as controlled by regional TC and terrain characteristics. Analysis of regional average footprints showed acceleration over windward slopes leading to some recovery of the abrupt wind speed reduction at the immediate coast. For risk management, this dataset may be used to better understand historical losses in regions of complex topography, and support the generation of synthetic event sets, particularly in regions of sparse historical data.

For large domains needed to capture the long tracks of fast-moving storms - over Japan or the Northeast U.S., for example - the simulation wall-clock time is substantially longer than using wind profile models alone. The most expensive domain, over Japan, at 900 x 1100 x 18 grid points using a 2-second timestep, a 24-hour simulation takes 6 hours wall-clock time on 36 cores. Smaller domains at a coarser 4-km grid spacing run much faster. This is efficient compared to the costs of high-resolution NWP simulations and therefore offer a computationally feasible approach to explore wind risk in complex terrain, while acknowledging that NWP models capture a fuller representation of terrain effects.

Other applications include real-time forecasting of overland TC winds in advance of approaching TCs. The model also may be used to produce wind exceedance probabilities (following a similar approach to that presented in Arthur (2019) and Arthur et al., 2008). High efficiency relative to numerical weather prediction (NWP) simulations, permits large numbers of simulations that could be used as inputs to a Generalized Extreme Value fit to the data to quantify the extremes. Another opportunity presented by this three-dimensional modelling of the boundary layer wind structure is an assessment of wind loading on high-rise structures. Today's coastal high-rise structures can extend above the surface layer into wind speeds far in excess of those at the surface (Vickery et al., 2009) at heights that are explicitly simulated in the model.

While the modelling approach captures more of the dynamics and physics of the TC boundary layer than analytical or empirical approaches, it misses a number of potentially important processes. A nonhydrostatic modelling system, for example, would capture more of the orographic effect (Wang, 2007). Perhaps more important is its accounting for only one-way of what is inherently a two-way interaction between the boundary layer and the free troposphere. For example, terrain variations can enhance convergence and trigger deep convection that may feedback on the low-level winds. TC responses to changes in land surface, such as at landfall, can have substantial effects on the whole TC circulations (e.g., Ramsay and Leslie, 2008; Wu, 2001). Another limitation is the use of a parametric TC wind profile model that is not designed to fit wind profiles of extratropical transitioning cyclones. During the process of transition, the wind field can become highly asymmetric and develop wind maxima on either side of the cyclone and far from the cyclone centre (e.g., Loridan et al., 2015). This presents a limitation of our modelling approach and may cause substantial errors in the footprints of strongly transitioning TCs over higher latitudes of the U.S. and Japan, for example. Finally, for wind loading and risk management application, an explicit representation of gusts is desirable.

Deleted: 3

This paper demonstrates the potential benefits of using a parametric wind-field model with a physical representation of terrain effects to model overland TC surface winds. Future work will explore the added value of this approach compared to the use of local wind multiplication factors. A more detailed process-level evaluation of terrain effects will identify the extent to which physical terrain effects are represented by this approach. Additional experiments should also explore sensitivity to model parameters such as model top height. Finally, future work should assess the value of this modelling technology and global landfalling TC catalogue in risk management decision making contexts.

- Deleted: d
- Deleted: incorporating
- Deleted: in a
- Deleted: computationally inexpensive
- Deleted: of
- Deleted: explore a
- Deleted: to
- Deleted: understand cause of the low wind speed bias over urban areas and more generally to
- Deleted: evaluate
- Deleted: in the model
- Deleted: F
- Deleted: also will

Author Contribution

- 10 JD, GH, IDW, SP and GS designed the investigation. YW led the methodology and software with contributions from JD and MG. MG ran the simulations, formal analysis, visualization and data curation. JD prepared the writing with contributions from all co-authors.

Competing Interests

- 15 The authors declare that they have no conflict of interest.

Data Availability

The Willis Research Network Global Tropical Cyclone Wind Footprint dataset version 1 will be made publicly available on the lead author's GitHub site on 1st May 2020. This time restriction follows terms of the funder, the Willis Research Network.

Acknowledgements

- 20 This work was funded by the Willis Research Network. The visit of Dr. Yuqing Wang to NCAR for the boundary layer model setup was partly supported by NCAR Mesoscale and Microscale Meteorology laboratory visitor funds. NCAR is sponsored by the National Science Foundation. We thank two anonymous reviewers and Bruce Harper for comments that greatly improved the manuscript.

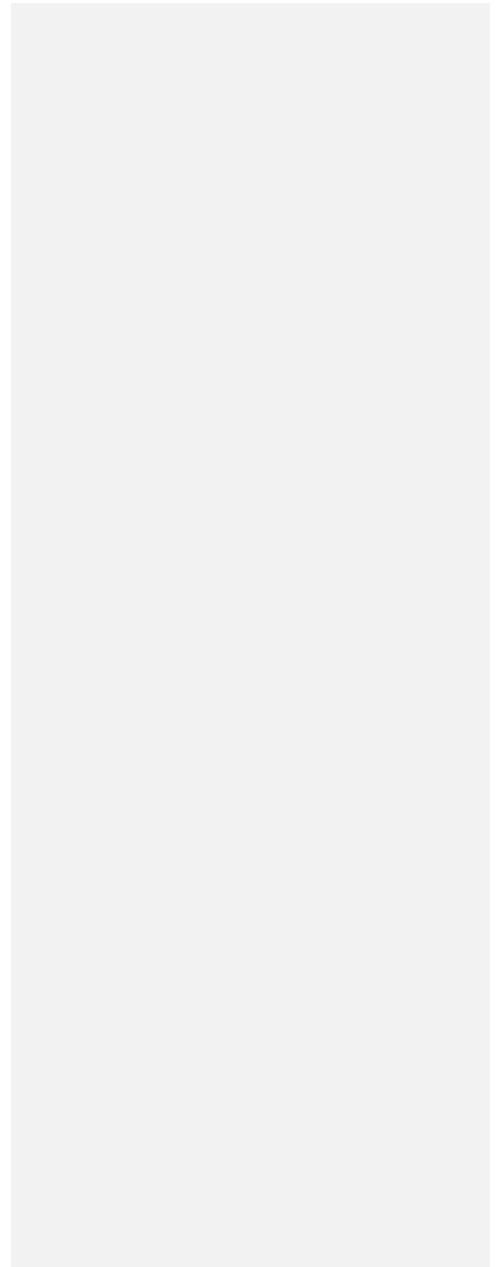
References

- [Arthur, W. C.: A statistical-parametric model of tropical cyclones for hazard assessment, Nat. Hazards Earth Syst. Sci. Discuss., <https://doi.org/10.5194/nhess-2019-192>, in review, 2019.](#)
- Arthur, W.C., Schofield, A., Cechet, R.P. and Sanabria, L.A.: Return period cyclonic wind hazard in the Australian region. In 28th AMS Conference on Hurricanes and Tropical Meteorology, 2008.
- Blackadar, A. K.: The vertical distribution of wind and turbulent exchange in a neutral atmosphere. *J. Geophys. Research*, 67(8), 3095-3102, <https://doi.org/10.1029/JZ067i008p03095>, 1962.
- Chavas, D. R., Reed, K. A. and Knaff, J. A.: Physical understanding of the tropical cyclone wind-pressure relationship. *Nature communications*, 8(1), p.1360, <https://doi.org/10.1038/s41467-017-01546-9>, 2017.
- Cobb, A. and Done, J. M.: The Use of Global Climate Models for Tropical Cyclone Risk Assessment. In: Collins J., Walsh K. (eds) *Hurricanes and Climate Change*. Springer, Cham, https://doi.org/10.1007/978-3-319-47594-3_7, 2017.
- Danielson, J.J. and Gesch, D.B.: Global multi-resolution terrain elevation data 2010 (GMTED2010) (No. 2011-1073). US Geological Survey, <https://doi.org/10.3133/ofr20111073>, 2011.
- Davis, C. A., Wang, W., Dudhia, J. and Torn, R.: Does increased horizontal resolution Improve hurricane wind forecasts? *Weather and Forecasting*, 25, 1826-1841, <https://doi.org/10.1175/2010WAF2222423.1>, 2010.
- Demuth, J., DeMaria, M. and Knaff, J. A.: Improvement of advanced microwave sounder unit tropical cyclone intensity and size estimation algorithms. *J. Appl. Meteor.*, 45, 1573-1581, <https://doi.org/10.1175/JAM2429.1>, 2006.
- Elsner, J. B., Kossin, J. P., Jagger, T. H.: The increasing intensity of the strongest tropical cyclones. *Nature* 455(7209):92-95, <https://doi.org/10.1038/nature07234>, 2008.
- Emanuel, K. A.: Increasing destructiveness of tropical cyclones over the past 30 years. *Nature* 436:686-688, <https://doi.org/10.1038/nature03906>, 2005.
- Estrada, F., Botzen, W. J. W., and Tol, R. S. J.: Economic losses from US hurricanes consistent with an influence from climate change. *Nat. Geosci.*, 8, 880-4, <https://doi.org/10.1038/ngeo2560>, 2015.
- [Franklin, J. L., Black, M. L., and Valde, K.: GPS dropwindsonde wind profiles in hurricanes and their operational implications. *Wea. Forecasting*, 18, 32-44, 2003.](#)
- Galperin, B., Kantha, L. H., Hassid, S., and Rosati, A.: A Quasi-equilibrium Turbulent Energy Model for Geophysical Flows. *J. Atmos. Sci.*, 45, 55-62, [https://doi.org/10.1175/1520-0469\(1988\)045<0055:AQETEM>2.0.CO;2](https://doi.org/10.1175/1520-0469(1988)045<0055:AQETEM>2.0.CO;2), 1988.
- Garratt, J. R.: Review of Drag Coefficients over Oceans and Continents. *Mon. Wea. Rev.*, 105, 915-929, [https://doi.org/10.1175/1520-0493\(1977\)105<0915:RODCOO>2.0.CO;2](https://doi.org/10.1175/1520-0493(1977)105<0915:RODCOO>2.0.CO;2), 1977.
- Geiger, T., Frieler, K. and Levermann, A.: High-income does not protect against hurricane losses. *Environmental Research Letters*, 11, 084012, [http://dx.doi.org/10.1061/\(ASCE\)1527-6988](http://dx.doi.org/10.1061/(ASCE)1527-6988), 2016.
- Giuliani, G. and Peduzzi, P.: The PREVIEW Global Risk Data Platform: a geoportal to serve and share global data on risk to natural hazards. *Natural Hazards and Earth System Science*, 11(1), 53-66, <https://doi.org/10.5194/nhess-11-53-2011>,

- 2011.
- Harper, B.A., Kepert, J.D. and Ginger, J.D.: Guidelines for converting between various wind averaging periods in tropical cyclone conditions. Geneva, Switzerland: WMO, 2010.
- Henderson, D., Ginger, J., Leitch, C., Boughton, G. and Falck, D.: Tropical Cyclone Larry: Damage to buildings in the
5 Innisfail area. CTS Tech. Rep. TR51, Cyclone Testing Station, School of Engineering, James Cook University, Townsville, QLD, Australia, 98 pp, 2006.
- Hill, K. A. and Lackmann, G. M.: The impact of future climate change on TC intensity and structure: A downscaling approach. *Journal of Climate* 24(17), 4644–4661, <https://doi.org/10.1175/2011JCLI3761.1>, 2011.
- Holland, G. J., and Bruyère, C.L.: Recent intense hurricane response to global climate change. *Climate Dynamics*, 42(3-4),
10 617–627, <https://doi.org/10.1007/s00382-013-1713-0>, 2014.
- Holland, G. J., Belanger, J. I. and Fritz, A.: A revised model for radial profiles of hurricane winds. *Monthly Weather Review*, 138, 4393–4401, <https://doi.org/10.1175/2010MWR3317.1>, 2010.
- [Holmes, J. D.: *Wind loading of structures*. 2nd ed. London and New York, Taylor & Francis, 2007.](#)
- Jakobsen, F. and H. Madsen, H.: Comparison and further development of parametric tropical cyclone models for storm surge
15 modeling. *Journal of Wind Engineering*, 92, 375–391, <https://doi.org/10.1016/j.jweia.2004.01.003>, 2004.
- Kepert, J. D.: Observed boundary-layer wind structure and balance in the hurricane core. Part I: Hurricane Georges. *J. Atmos. Sci.*, 63, 2169–2193, <https://doi.org/10.1175/JAS3745.1>, 2006a.
- Kepert, J. D.: Observed boundary-layer wind structure and balance in the hurricane core. Part II: Hurricane Mitch. *J. Atmos. Sci.*, 63, 2194–2211, , <https://doi.org/10.1175/JAS3746.1>, 2006b.
- 20 Kepert, J. D.: Choosing a boundary layer parameterization for tropical cyclone modelling. *Monthly Weather Review* 140, 1427–1445, <https://doi.org/10.1175/MWR-D-11-00217.1>, 2012.
- Kepert, J. D. and Wang, Y.: The Dynamics of Boundary Layer Jets within the Tropical Cyclone Core. Part II: Nonlinear Enhancement. *J. Atmos. Sci.*, 58, 2485–2501, [https://doi.org/10.1175/1520-0469\(2001\)058<2485:TDOBLJ>2.0.CO;2](https://doi.org/10.1175/1520-0469(2001)058<2485:TDOBLJ>2.0.CO;2), 2001.
- [Knaff, J.A., DeMaria, M., Molenaar, D.A., Sampson, C.R., Seybold, M.G.: An Automated, Objective, Multiple-Satellite-
25 Platform Tropical Cyclone Surface Wind Analysis.” *Journal of Applied Meteorology and Climatology* 50 \(10\): 2149–66, 2011.](#)
- Knapp, K., Kruk, M. C., Levinson, D. H., Diamond, H. J. and Neumann, C. J.: The International Best Track Archive for Climate Stewardship (IBTrACS). *Bull. Amer. Meteor. Soc.*, 91, 363–376, <https://doi.org/10.1175/2009BAMS2755.1>, 2010.
- Loridan, T., Khare, S., Scherer, E., Dixon, M. and Bellone, E.: Parametric modeling of transitioning cyclone wind fields for risk assessment studies in the western North Pacific. *J. Appl. Meteor. Climatol.*, 54, 624–642, <https://doi.org/10.1175/JAMC-D-14-0095.1>, 2015.
- 30 Loridan, T., Crompton, R. P. and Dubossarsky, E.: A Machine Learning Approach to Modeling Tropical Cyclone Wind Field Uncertainty. *Mon. Wea. Rev.*, 145, 3203–3221, <https://doi.org/10.1175/MWR-D-16-0429.1>, 2017.

- Meng, Y., Matsui, M. and Hibi, K.: A numerical study of the wind field in a typhoon boundary layer. *Journal of Wind Engineering and Industrial Aerodynamics* 67–68: 437–448, [https://doi.org/10.1016/S0167-6105\(97\)00092-5](https://doi.org/10.1016/S0167-6105(97)00092-5), 1997.
- Miller, C., Gibbons, M., Beatty, K. and Boissonnade, A.: Topographic speed-up effects and observed roof damage on Bermuda following Hurricane Fabian (2003). *Weather and Forecasting*, 28(1), pp.159-174, <https://doi.org/10.1175/WAF-D-12-00050.1>, 2013.
- Mitchell-Wallace, K., Foote, M., Hillier, J. and Jones, M.: *Natural catastrophe risk management and modelling: A practitioner's guide*. John Wiley & Sons, <https://doi.org/10.1002/9781118906057>, 2017.
- Murakami, H., Wang, Y., Yoshimura, H., Mizuta, R., Sugi, M., Shindo, E., Adachi, Y., Yukimoto, S., Hosaka, M., Kusunoki, S. and Ose, T.: Future changes in tropical cyclone activity projected by the new high-resolution MRI-AGCM. *Journal of Climate*, 25(9), 3237-3260, <https://doi.org/10.1175/JCLI-D-11-00415.1>, 2012.
- NCEP/NWS/NOAA/U.S. Department of Commerce.: *NMC ADP Global Surface Observations Subsets*. Research Data Archive at the National Center for Atmospheric Research, Computational and Information Systems Laboratory. <https://doi.org/10.5065/BARE-NP34>, 1995. Last accessed Feb 1, 2019.
- 15 Pielke Jr, R. A., Gratz, J., Landsea, C. W., Collins, D., Saunders, M. A. and Musulin, R.: Normalized hurricane damage in the united states: 1900–2005. *Natural Hazards Review*, <https://doi.org/10.1061/ASCE1527-698820089>, 2008.
- Powell, M. D. and Houston, S. H.: Surface wind fields of 1995 Hurricanes Erin, Opal, Luis, Marilyn, and Roxanne at landfall. *Mon. Wea. Rev.*, 126, 1259–1273, [https://doi.org/10.1175/1520-0493\(1998\)126<1259:SWFOHE>2.0.CO;2](https://doi.org/10.1175/1520-0493(1998)126<1259:SWFOHE>2.0.CO;2), 1998.
- Powell, M. D., Houston, S. H., Amat, L. R. and Morisseau-Leroy, N.: The HRD real-time hurricane wind analysis system. *J. Wind Engineer. and Indust. Aerodyn.* 77&78, 53-64, [https://doi.org/10.1016/S0167-6105\(98\)00131-7](https://doi.org/10.1016/S0167-6105(98)00131-7), 1998.
- 20 Powell, M. D., Vickery, P. J. and Reinhold, T. A.: Reduced drag coefficient for high wind speeds in tropical cyclones. *Nature*, 422, 279–283, <https://doi.org/10.1038/nature01481>, 2003.
- Ramsay, H. A. and Leslie, L. M.: The effects of complex terrain on severe landfalling Tropical Cyclone Larry (2006) over northeast Australia. *Mon. Wea. Rev.*, 136, 4334–4354, <https://doi.org/10.1175/2008MWR2429.1>, 2008.
- 25 Ramsay, H. A., Leslie, L. M. and Kepert, J. D.: A high-resolution simulation of asymmetries in severe Southern Hemisphere Tropical Cyclone Larry (2006). *Monthly Weather Review*, 137(12), 4171–4187, <https://doi.org/10.1175/2009MWR2744.1>, 2009.
- Ranson, M., Kousky, C., Ruth, M., Jantarasami, L., Crimmins, A. and Tarquinio, L.: Tropical and extratropical cyclone damages under climate change. *Climatic change*, 127(2), 227-241, <https://doi.org/10.1007/s10584-014-1255-4>, 2014.
- 30 Schwendike, J. and Kepert, J. D.: The boundary layer winds in Hurricanes Danielle (1998) and Isabel (2003). *Mon. Wea. Rev.*, 136, 3168–3192, <https://doi.org/10.1175/2007MWR2296.1>, 2008.
- Smith, S. D.: Coefficients for sea surface wind stress, heat flux, and wind profiles as a function of wind speed and temperature. *J. Geophys. Res.* 93, 15467–15472, <https://doi.org/10.1029/JC093iC12p15467>, 1988.

- Smith, A. and Katz, R.: U.S. Billion-dollar Weather and Climate Disasters: Data Sources, Trends, Accuracy and Biases. *Natural Hazards*, <https://doi.org/10.1007/s11069-013-0566-5>, 2013.
- Tan, C. and Fang, W.: Mapping the wind hazard of global tropical cyclones with parametric wind field models by considering the effects of local factors. *International Journal of Disaster Risk Science*, 9(1), 86-99, <https://doi.org/10.1007/s13753-018-0161-1>, 2018.
- Vickery, P. J., Masters, F. J., Powell, M. D. and Wadhera, D.: Hurricane hazard modeling: The past, present, and future. *Journal of Wind Engineering and Industrial Aerodynamics*, 97(7-8), 392-405, <https://doi.org/10.1016/j.jweia.2009.05.005>, 2009.
- Villarini, G., and Vecchi, G. A.: Projected increases in North Atlantic tropical cyclone intensity from CMIP5 models. *Journal of Climate* 26(10), 3231-3240, <https://doi.org/10.1175/JCLI-D-12-00441.1>, 2013.
- Walsh, K. J., McBride, J. L., Klotzbach, P. J., Balachandran, S., Camargo, S. J., Holland, G., Knutson, T. R., Kossin, J. P., Lee, T. C., Sobel, A. and Sugi, M.: Tropical cyclones and climate change. *Wiley Interdisciplinary Reviews: Climate Change*, 7(1), 65-89, <https://doi.org/10.1038/ngeo779>, 2016.
- Wang, Y.: A multiply nested, movable mesh, fully compressible, nonhydrostatic tropical cyclone model – TCM4: Model description and development of asymmetries without explicit asymmetric forcing. *Meteor. Atmos. Phys.*, 97, 93-116, <https://doi.org/10.1007/s00703-006-0246-z>, 2007.
- Weinkle, J., Maue, R. and Pielke Jr, R.: Historical global tropical cyclone landfalls. *Journal of Climate*. 25(13), 4729–4735, <https://doi.org/10.1175/JCLI-D-11-00719.1>, 2012.
- Wu, C. C.: Numerical simulation of Typhoon Gladys (1994) and its interaction with Taiwan terrain using the GFDL hurricane model. *Mon. Wea. Rev.*, 129, 1533–1549, [https://doi.org/10.1175/1520-0493\(2001\)129<1533:NSOTGA>2.0.CO;2](https://doi.org/10.1175/1520-0493(2001)129<1533:NSOTGA>2.0.CO;2), 2001.
- [Yang, T., Cechet, R.P. and Nadimpalli, K.: Local wind assessment in Australia: Computation methodology for wind multipliers. *Geoscience Australia*. 2014/33, 2014.](#)
- Youngman, B.D. and Stephenson, D. B.: A geostatistical extreme-value framework for fast simulation of natural hazard events, *Proceedings of the Royal Society A: Mathematical, Physical and Engineering Sciences*, volume 472, no. 2189, <https://doi.org/10.1098/rspa.2015.0855>, 2016.
- [Willoughby, H.E., Darling, R.W.R. and Rahn, M.E.: Parametric representation of the primary hurricane vortex. Part II: A new family of sectionally continuous profiles. *Monthly Weather Review*, 134\(4\), 1102-1120, 2006.](#)
- [Zhang, B., Perrie, W., Zhang, J.A., Uhlhorn, E.W. and He, Y.: High-resolution hurricane vector winds from C-band dual-polarization SAR observations. *Journal of Atmospheric and Oceanic Technology*, 31\(2\), 272-286, 2014.](#)
- Zhang, J.A., Rogers, R.F., Nolan, D.S. and Marks Jr, F.D.: On the characteristic height scales of the hurricane boundary layer. *Monthly Weather Review*, 139(8), 2523-2535, <https://doi.org/10.1175/MWR-D-10-05017.1>, 2011.
- [Zhang, J.A., Drennan, W.M., Black, P.G., and French, J.R.: Turbulence structure of the hurricane boundary layer between the outer rainbands. *J. Atmos. Sci.*, 66, 2455–2467, 2009.](#)



Page 13: [1] Deleted	James Done	11/19/19 10:54:00 AM
-----------------------------	-------------------	-----------------------------

Page 13: [2] Deleted	James Done	10/21/19 9:15:00 AM
-----------------------------	-------------------	----------------------------

